LATE QUATERNARY STRATIGRAPHY AND INFILLING OF THE MEGHNA RIVER VALLEY

ALONG THE TECTONICALLY ACTIVE EASTERN MARGIN OF THE GANGES-

BRAHMAPUTRA-MEGHNA DELTA

By

Lauren A. Williams

Thesis

Submitted to the Faculty of the

Graduate School of Vanderbilt University

in partial fulfillment of the requirements

for the degree of

MASTER OF SCIENCE

in

Earth & Environmental Science

May 2014

Nashville, Tennessee

Approved:

John Ayers, Ph.D.

Steven L. Goodbred, Jr, Ph.D.

To my parents, John and Cheryl, and my sisters, Libby and Bridget,

for your life-long support of my pursuits

and to VUDU for all of your vlove

ACKNOWLEDGEMENTS

TABLE OF CONTENTS

LIST OF TABLES

Table

LIST OF FIGURES

Figure

Chapter I

Introduction

A. Motivation

Insights into how tectonics, alluvial channels, and sediment interact to build the stratigraphy in a tectonically active depositional basin can be discovered by studying the system's sediment record and geomorphology. Tectonic influence on basin systems are often overlooked due to more dominant controls such as sea level, climate, and sediment load. In the absence of tectonic deformation, elevation gradients generated through vertical aggradation and the construction of stratigraphy and internal feedbacks can cause fluvial channels to migrate, rapidly change course, or avulse (Jones and Schumm, 1999). Similarly, tectonic deformation can tilt the landscape and steer the fluvial channel, thus controlling the composition and location of channel deposits.

Many studies have examined tectonic control on modern fluvial systems using planform morphometrics such as channel sinuosity and location. For example Ouchi (1985) compared responses to uplift and tilting obtained in experimental braided and meandering channel models to the Rio Grande, San Joaquin, and the Texas Coast rivers. Another group of studies compared the rate of tectonic tilting to the resultant style of channel movement, including Nanson (1980) for the Beatton River, Leeder and Alexander (1987) for the Madison, South Fork, and Mississippi rivers, Reid (1992) for the Owens River, and Holbrook and Schumm (1999) for the Jefferson River. Shifts in channel drainage networks in response to tectonic deformation have also been noted along the the Yenisei, Ob, and Irtysh rivers (Allen and Davies, 2007). Kim et al. (2010) sought to model physically the steering of fluvial channels through tectonic tilt. Some authors highlight that insight can be gained from looking at the sediment record (Holbrook and Schumm, 1999), but there is a lack of studies that evaluate tectonic controls through deciphering the recent stratigraphy in a fluvial system.

From the sediment record, establishing channel history and channel behavior, including avulsions, migration, and overbank processes, is the key to investigating how rivers and tectonics interact to shape the landscape. The necessary components for capturing channel behavior in the stratigraphic record are a subsiding basin generating storage capacity, a sufficient sediment load, and a fluvial system capable of transporting the sediment. The site for this study, the Ganges Brahmaputra Meghna Delta (GBMD), is a basin that is capable of capturing sediment with sufficient fluvial channels and sediment load to produce a complete record of past channel behavior. This study looks at whether tectonic deformation can be the primary control on fluvial geomorphology and channel behavior. It specifically seeks to find tectonic influence on short enough timescales to be identified in the sedimentary record of the late Pleistocene to the present in proximity to a convergent boundary which is tilting the land surface in a tectonically active basin.

B. Background

i. Rivers and tectonics

Tectonics can influence rivers in numerous significant ways as Schumm et al. describe in *Active Tectonics and Alluvial Rivers* (2000) and *River Variability and Complexity* (2005). Tectonic influences on river behavior and morphology can originate upstream of a basin or locally along a particular fluvial reach. An example of an upstream influence would be an increase in coarse sediment load due to uplift, or a disturbance that is either gradual or from a major seismic event, which mobilizes sediment from hillslopes into river valleys. At the local level, tectonic deformation can change the bed slope along the channel or the lateral tilt if deformation is applied across the channel (Holbrook and Schumm, 1999). In the Meghna valley, deformation of the up to 17 km thickness of sediment in the Bengal basin results in low amplitude folds with axes roughly parallel to channel flow (Uddin and Lundberg, 2003; Sikder and Alam 2003). A change in channel slope will evoke an adjustment of the channel; and such adjustments depend on whether tilting is lateral or longitudinal to the channel. In the case of lateral tilting, which can occur from low amplitude folding, the river may avulse or migrate based on the net change in gradient

2

and the rate of the tilting in relation to other system factors controlling sedimentation (Schumm et al.,

2000). A large change in channel-bed gradient over a short period of time is more likely to trigger an

avulsion, which could result from gradual bed aggradation or a single tectonic event (Schumm et al.,

2000). The other response to lateral tilting is channel migration or 'combing', which occurs when the tilt

rate is not fast enough to cause an avulsion. Typical lateral tilting rates that favor migration over avulsion

are 2-3 orders of magnitude less than the avulsion tilt rate, whose average is $\geq 7.5 \times 10^{-3}$ radians ka^{-1}, which

mean tilt rates that favor migration are $\leq 10^{-5}$ radians ka^{-1} (Schumm et al., 2000).

Physical modeling of channel behavior in response to active tectonics has been used to determine

resulting sedimentary architecture and landscape changes that might be recongized in modern systems

(Ouchi, 1985; Kim et al., 2010). The experiments of Kim et al. (2010) demonstrated that two timescales

are important for tectonic steering of channels, including (i) the lateral channel mobility timescale, T_c,

which is the time it takes for the channel to visit all areas of the valley, and (ii) the tectonic deformation

timescale, T_t, which is the time it takes for the channel to tilt enough to steer channel flow. The ratio

between these timescales needs to be sufficiently large for the channel to respond to tectonic deformation

(T_c/T_t). Without a large enough ratio between the timescales, the river channel would be immobilized due

to uplift and incision. For a channel to migrate in response to lateral tilting, it is also important to have a

ratio between the downstream channel slope (S_x) and the cross-channel slope (S_y) that is small ($S_x/S_y \leq$

0(1)).

ii.   Ganges Brahmaputra Meghna Delta

The GBMD is formed by three principal fluvial systems - the Ganges, Brahmaputra, and Meghna

- that transport a sediment load of ~1 x 10^9 t/yr across an area of active tectonics involving the

convergence of three tectonic plates- Indian, Burman, and Eurasian that has resulted in the formation of

the Bengal Basin, a site of continued deformation and sediment deposition (fig. 1,2) (Goodbred et al.,

2003; Steckler et al., 2008). The Ganges and Brahmaputra drain the Himalayas and account for roughly

3

90% of basin discharge while smaller rivers, the Barak, Surma, and Kushiara, join to form the Meghna river and drain the Indo-Burman ranges east of the GBMD (fig. 3). The Brahmaputra river has a history of avulsions between two main courses, its western Jamuna course and the eastern Old Brahmaputra course, which has been documented in the sediment record and in historical records (fig. 4) (Fergusson, 1863; Oldham, 1899; Goodbred and Kuehl 2000; Best et al., 2007; Pickering et al., 2013).
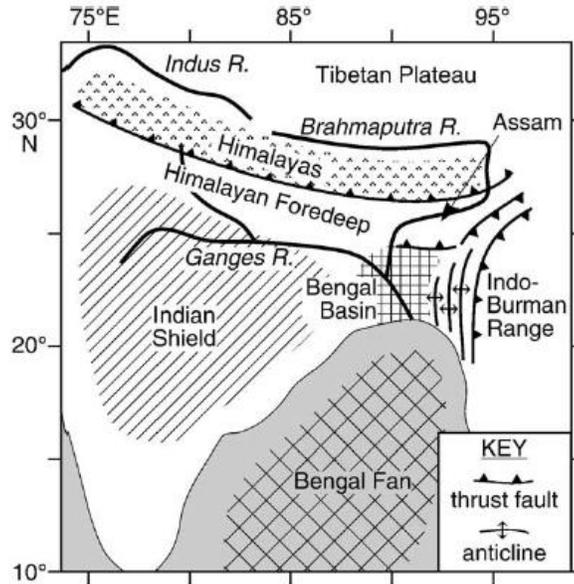
1A.
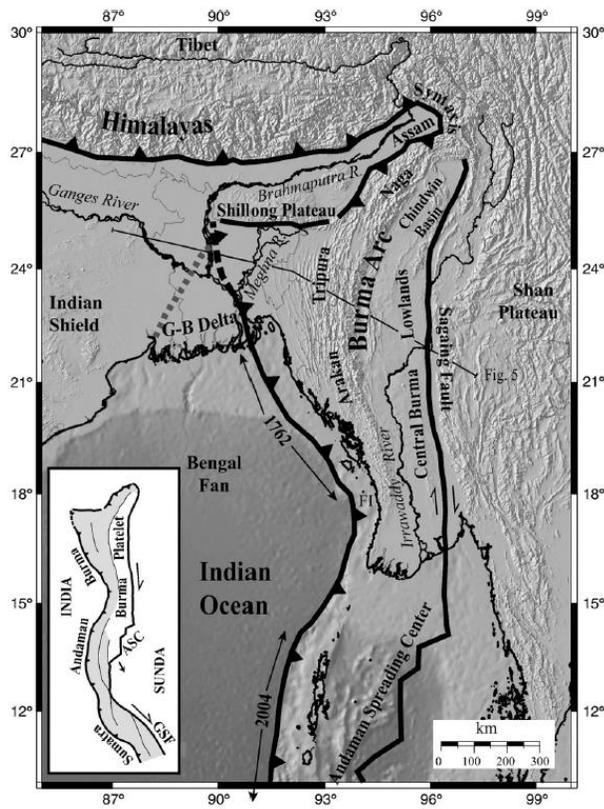
1B.

Figure 1A. Tectonic and sedimentary map of the Indo-Asian collision. Active tectonics and sediment deposition interact in the Bengal Basin due to the convergence of tectonic plates resulting in faulting and deformation with a large sediment load concurrently coming from the uplift of the Himalayas and being transported by the large rivers. Sediment is deposited as active tectonics deform the landscape (Goodbred et al., 2003). 1B. Topographic map with tectonic features of Indo-Eurasian collision— major faults and tectonic boundaries are marked by heavy black lines. Note the dotted gray line within the G-B Delta that marks the estimated location of the hinge-line of the Indo-Burman convergence. The area to the east of the hinge-line and to the west of the thrust is an area of sediment undergoing active deformation (Steckler et al., 2008).
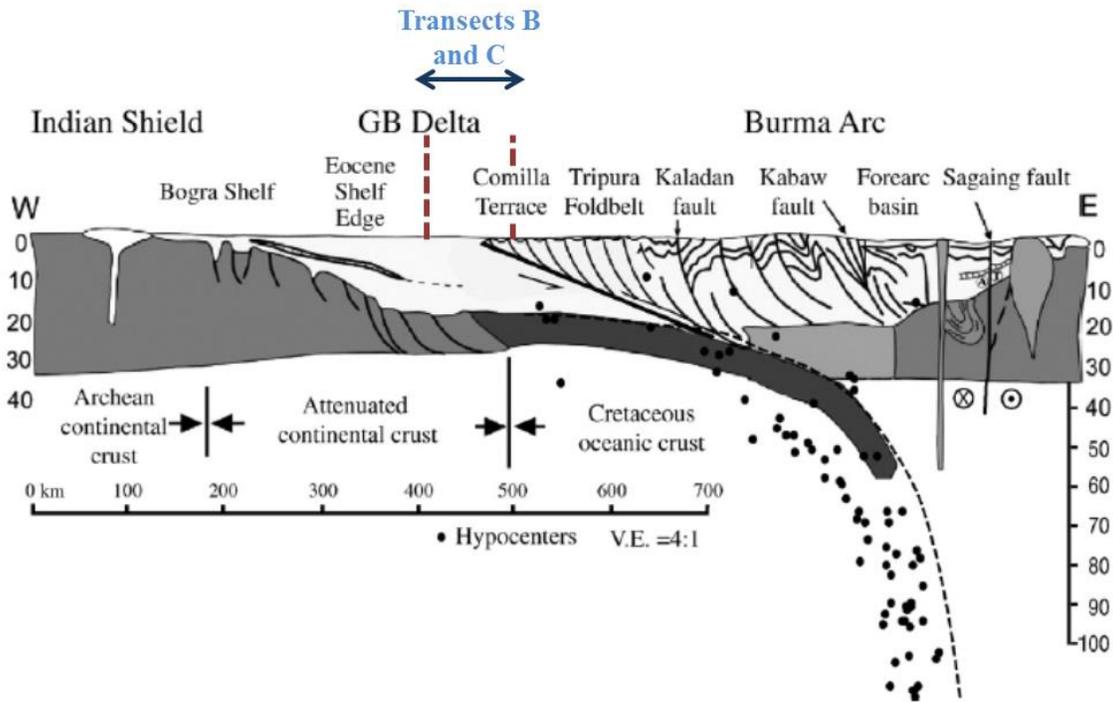
Figure 2. Structural cross section. Cross section extending from the Indian Shield to the Burma Arc across the GBMD system with the proposed study area marked as Transects B and C. The GB Delta consists of a 10-20 km of sediment sourced from the Himalayas deposited by alluvial channels. This thick pile of sediment undergoes deformation in the form of folding and thrusting from the active tectonics at the convergence of the Indian and Burman tectonic plates that form a low angle subduction zone (Steckler et al., 2008).
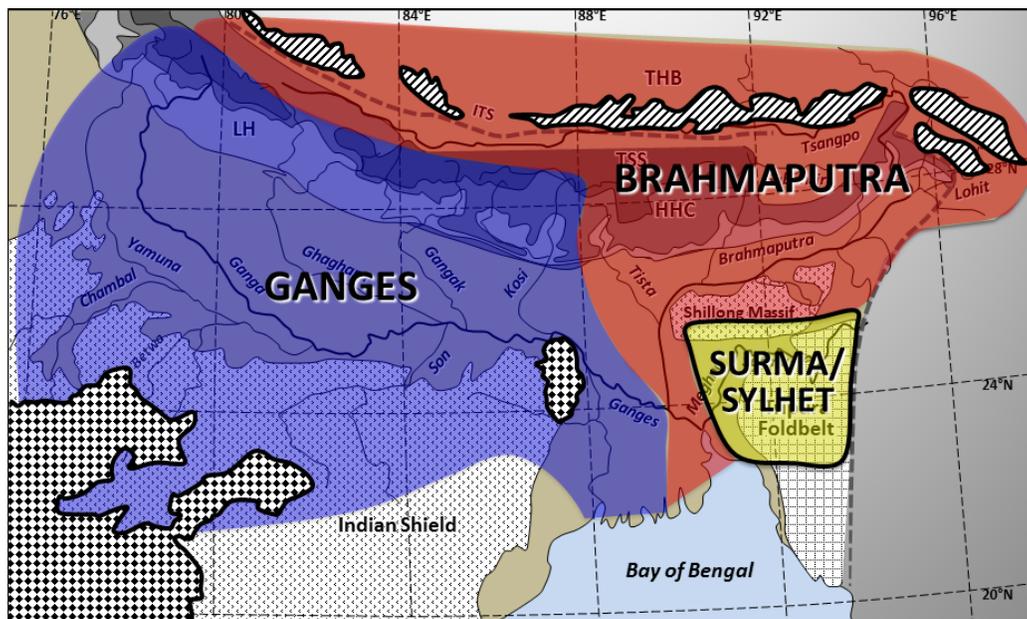
Figure 3. River drainage map. The river drainages areas that source sediment into of the Ganges Brahmaputra Meghna Delta (Goodbred, *in press*).
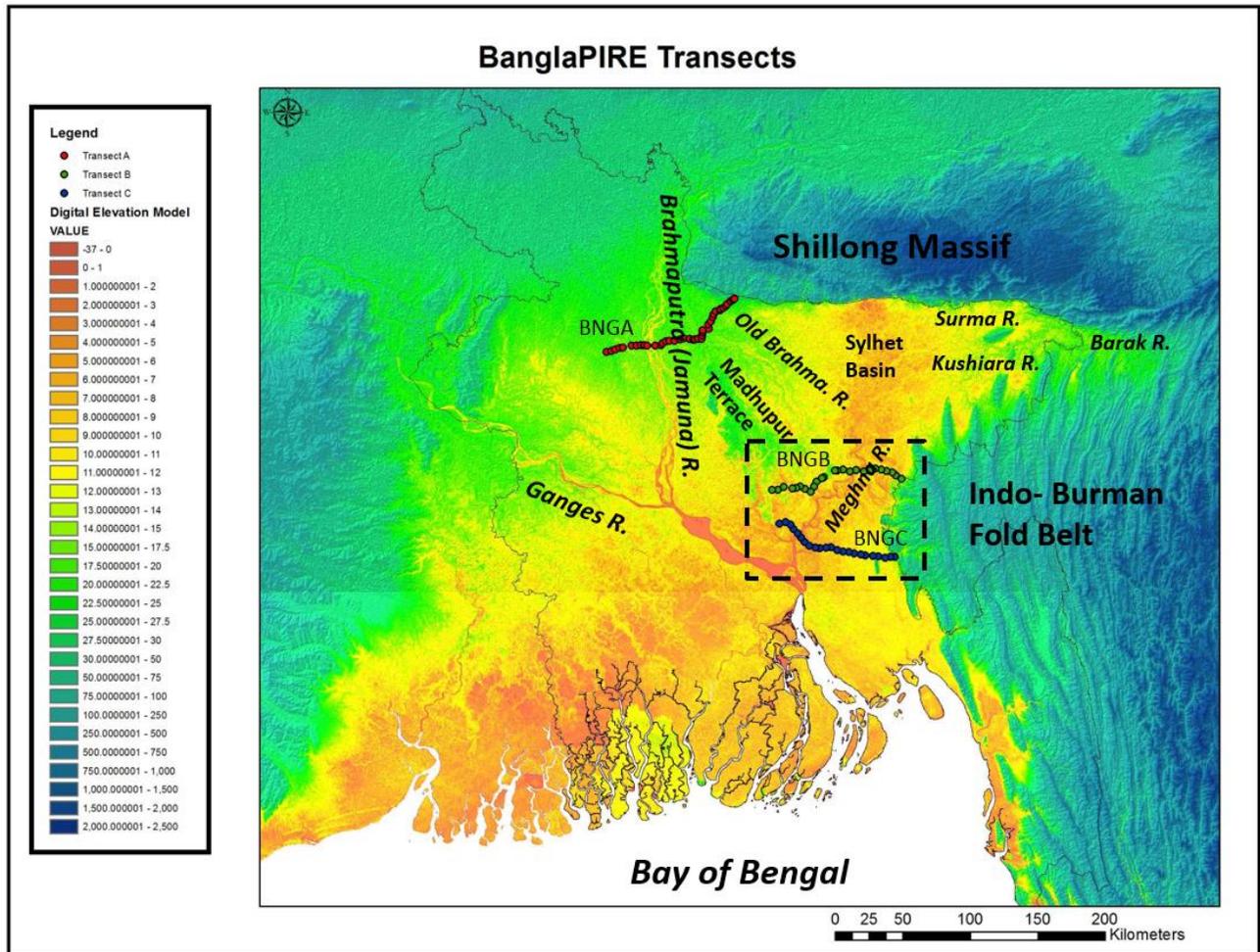
Figure 4. DEM area map of Ganges Brahmaputra Meghna Delta. Core transects from Pickering et al. (2013)- BNGA and for this study- BNGB and BNGC are marked on the map. The Meghna valley study area is in the black dashed box.

The ongoing uplift and erosion of the Himalayas has built out the GBMD for the last ~40 m.y., since the collision of the Indian and Eurasian plates, making it the world's largest subaerial delta system at ~100,000 km^2 in area with sediment thicknesses up to 17 km (Goodbred et al., 2003; Steckler et al., 2008). A subsidence rate for the GBMD of 2-4 mm/yr generates accommodation space allowing for preservation of the sediment record with a lack of reworking (Goodbred et al., 2003). The GBMD is controlled tectonically on two scales, (a) sediment provision: the northward Indian plate movement causes the Himalayan uplift on the edge of the Bengal margin that provides a large amount of coarse sediment to the rivers and (b) deformation: the eastward Indian plate movement deforms the Bengal Basin and leads to growth of the low-amplitude Indo-Burman fold belt, which blindly extends into the delta and continues to develop through overthrusting and compression (fig. 2) (Goodbred et al., 2003; Steckler et al., 2008).

This study is part of a larger research effort, the BanglaPIRE project, which seeks to better define the intersection of tectonics and fluvial systems by studying the GBMD. The first drilling effort of the BanglaPIRE project, transect BNGA, focused on the avulsion node of the Brahmaputra River between its Jamuna and Old Brahmaputra courses and consisted of 41 boreholes along a 120 km long transect (fig. 4,5) (Pickering et al., 2013). Grain size, strontium concentration, and magnetic susceptibility aided in characterizing the sediment from the late Pleistocene through Holocene which furthered understanding of behavior of the fluvial channel and its recent avulsion history (fig. 5). The channel deposits from the Brahmaputra River, both Holocene and Pleistocene, were found to have higher strontium concentration and higher magnetic susceptibility than local sediment sources from the Shillong Massif, Tista Fan, and Madhupur Terrace that flank the sides of the main alluvial valleys (fig. 4 and 5). Confidence in our ability to differentiate the various sediment sources such as the Brahmaputra prompted the current study, which drilled core transects BNGB and BNGC at locations downstream along the Brahmaputra's eastern course via Sylhet basin and the Meghna valley, the latter of which traverses an active deformation front (fig. 4).
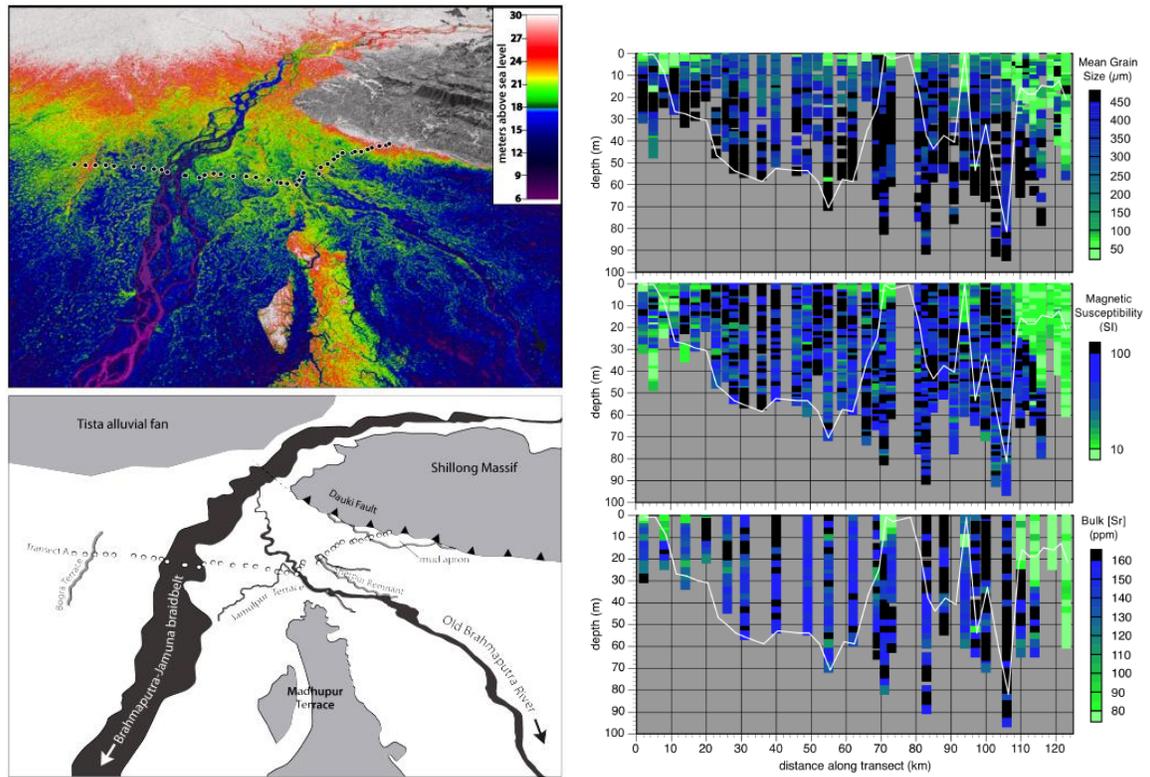
Figure 5. BNGA map and summary of results. The BNGA drilling transect is at the avulsion node for the Brahmaputra River between the western or Jamuna course and the eastern course or the Old Brahmaputra course. The plots on the right show the data set from BNGA. On the top is grain size, the middle plot is magnetic susceptibility, and the bottom plot is strontium concentration.

iii. Geomorphic provinces in the Meghna valley

The Madhupur terrace, an elevated surface of Pleistocene-age delta sediments, bounds the Meghna valley to the west (fig. 4, 6). Drill cores collected from this area were located in small, local valleys that incise the Madhupur terrace. East of the terrace, transects BNGB and BNGC traverse the Meghna River channel, which is ~3-15 km wide and up to 20-25 m deep. The physiography of BNGB can be divided into two principal valleys by a remnant portion of the Madhupur terrace, with smaller shallower channels on the western side and the main Meghna channel on the eastern side with its termination at a river cut margin of Pleistocene hills along the Indo-Burman fold belt. In contrast, the main valley along transect BNGCis wider and not partitioned in to small sub-valleys; it extends from the eastern margin of Madhupur terrace to the active, young Tippera surface that is highlighted by the outcropping Lalmai anticline towering over the subtle landscape (fig. 6, 7). The Tippera surface has a gradient of ~2.5 x 10^{-4} sloping upwards toward the fold belt. To the east of the Lalmai anticline along BNGC, the valleys locally drain the fold belt from east to west towards Lalmai anticline and the Meghna channel.
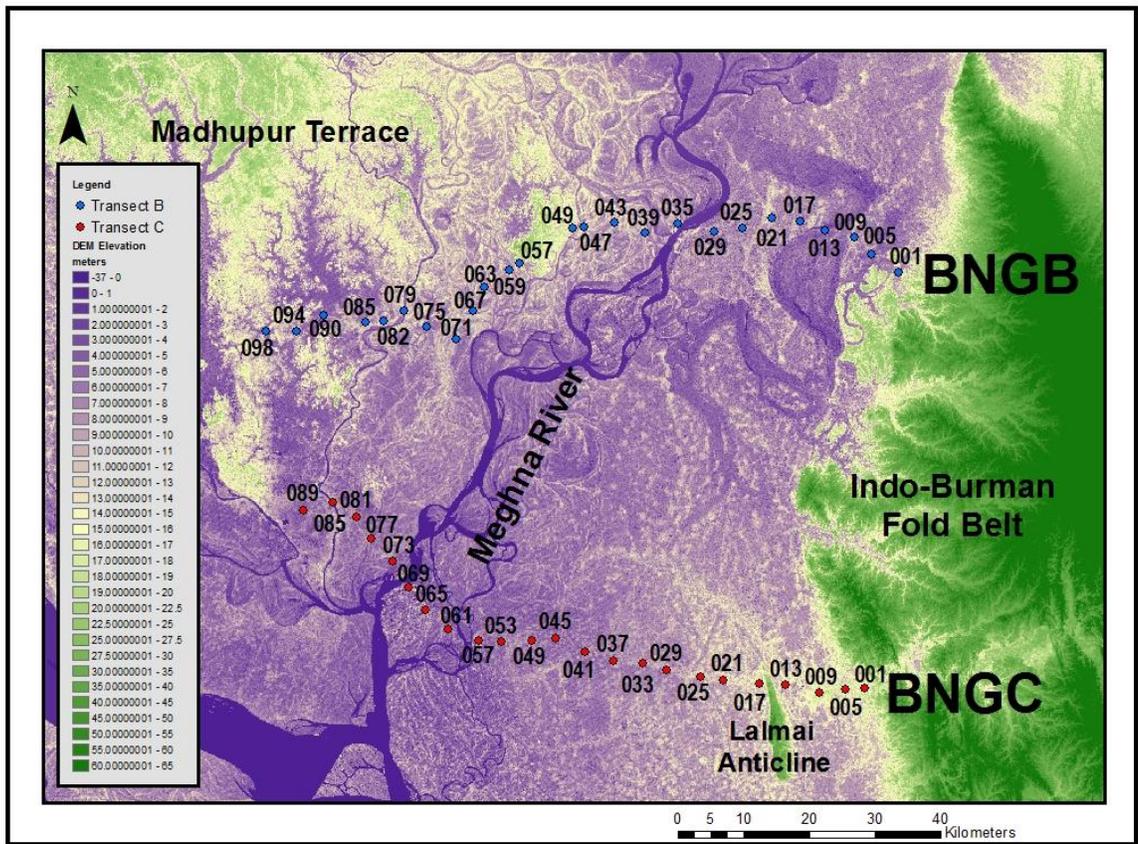
Figure 6. BNGB and BNGC core locations and geologic setting.
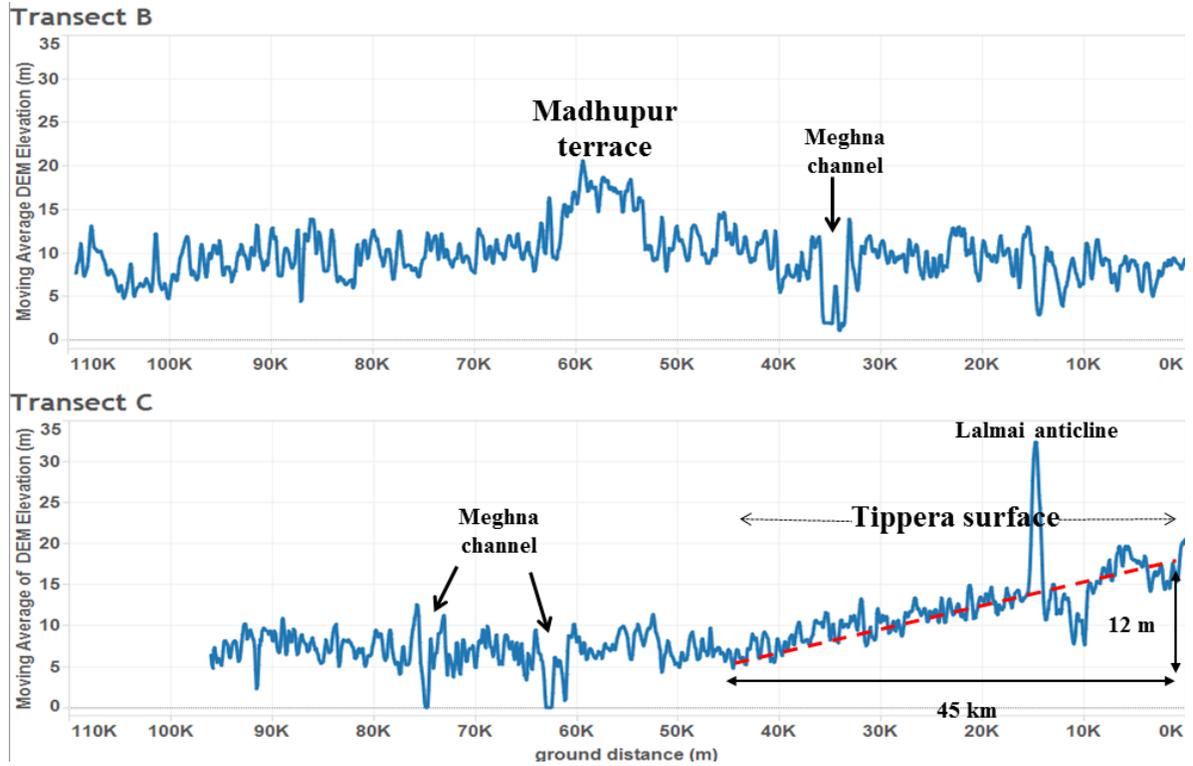
Figure 7. Cross channel profiles of BNGB and BNGC. BNGB shows almost no gradient while BNGC's eastern side has a gradient of ~2.5 x 10^{-4} from the valley floor upwards to the fold belt. Elevation data is from SRTM data.

Chapter II

Approach and Methods

A. Site selection

The Meghna valley was chosen to investigate the role of tectonic deformation on fluvial processes and delta development due to its location alongside the Indo-Burman fold belt (fig. 4). Observed convergence and deformation of the GBMD occurs as folds propagate westward into the Bengal basin (Sikder and Alam 2003; Uddin and Lundberg, 2004; Steckler et al., 2008) and the repeated occupation and abandonment by the Brahmaputra River make the Meghna River valley an ideal place to study tectonic sediment interactions. The Meghna valley is also fed by a confluence of smaller rivers draining the Shillong Massif and Indo-Burman ranges, including the Barak, Surma, and Kushiara (BSK) rivers that converge through the Meghna valley (fig. 4). Therefore, stratigraphy of the Meghna valley records periods when the valley is occupied by both the BSK rivers and the Brahmaputra River and the extent of input from more local sources from Madhupur terrace and the Indo-Burman fold belt. Furthermore, sediments transported by the Brahmaputra and BSK rivers are geochemically distinct (Goodbred et al, *in press*), providing the opportunity to reconstruct the history of channel location, occupation time, and sedimentation rate contributed by the two rivers systems.

B. Sampling

Forty-eight boreholes with ~3-4 km spacing were drilled along two transects, BNGB and BNGC (fig. 5) using a local well drilling method that employs a bamboo fulcrum and lever system with PVC drill pipe. The rig is operated by a crew of 3-4 drillers who can complete one borehole per day to depths of 50 m up to 100 m. The drilling method is as simple as using the driller's hand as a check valve over PVC tubing and catching the wash borings as they are extruded from the drill pipe. For this study samples were collected at 1.5 m intervals, or at half intervals if there was a lithology change detected by the driller. Sand sized sediments are extruded from the drill pipe as a slurry, whereas mud deposits are

13

cohesive and extruded as coherent plugs. Collected sediments are described in the field for color, plasticity and organic material, that latter of which is preserved separately for radiocarbon dating.

C. Sediment analysis

The characteristics of the borehole samples- color, grain size, plasticity, radiocarbon dates, sediment geochemistry, and magnetic susceptibility- reveal attributes such as river sediment lithology, current velocities, depositional energy and environment of deposition, and history of burial in the stratigraphic record. Combining these sedimentological attributes can be used to define facies that reflect environments or particular processes within the study area. The temporal and spatial distribution of these facies within the stratigraphy are used to define the paleoenvironmental history of river-delta-tectonic interactions.

i. Color

Sediment color was determined in the field using a standardized color chart. Results are used as a general proxy for the oxidation state and degree of weathering of sediment. Tan, orange, to reddish sediment indicate oxidative weathering in the vadose zone prior to burial below the water table. Darker, gray to black sediments reflect reducing depositional settings or groundwater environments that may be finer-grained and included higher organic carbon contents, which were tested by loss-on-ignition (LOI). Color variations may also be used, with care, to correlate stratigraphic horizons between boreholes.

ii. Grain size

Grain size was noted qualitatively in the lithologic description at time of sampling. Quantitative measures of grain size was conducted for 171 samples using the Malvern Mastersizer laser-diffraction particle-size analyzer. The Malvern system measures particle size distributions from 0.5-1100 μm. Grain size yields channel facies information and distance from the sediment source. Medium to coarse sand bodies are likely from the thalweg and finer sands from channel levees and bars both indicating channel

14

location. Silt and clay sized particle comprising mud deposits are from either overbank flow where found in meter-scale deposits or as basinal deposits where found in thicknesses greater than several meters. Overbank deposits are associated with nearby channel flooding, while basinal mud deposits are associated with deposition away from the main river channels, which excludes sand input and thus only sustains fine sediment accumulation.

iii. Plasticity

The plasticity of cohesive mud deposits can be a useful indicator of the degree of desiccation, compaction, and weathering that has occurred since deposition, and thus provides a proxy for relative age and subaerial exposure of sediments. The plasticity of mud samples are noted in the field, with samples of low plasticity recognized as being stiff and non-deformable. These stiff samples in the GBMD generally reflect buried soil horizons in which pore space has been partially filled through pedogenic alteration and formation of clays, amorphous silica and iron oxyhydroxides (Pickering et al., 2013). Such alteration occurs through oxidative vadose zone weathering and is a good indicator of lowstand exposure surfaces, when deposition on the delta largely ceases as the rivers become incised. An associated lab study using SEM and XRD identified that low plasticity muds have void space infilled by amorphous silica most likely raising the density and lowering porosity, but density and porosity cannot be specifically determined due to our coring method (Pickering, J., pers. comm., December 15, 2012).

iv. Radiocarbon

Coring of preserved stratigraphy locally yielded organic-rich sediments with macroscopic fragments of woods and grasses. Dates from radiocarbon samples indicate timing of sediment deposition under the assumption that the organic carbon has not been reworked from older deposits. Organic material found in muddy, organic-rich sediments are likely not reworked due to rapid degradation and lack of preservation of organic material in sediments that have been reworked. Also wood found in sand

has been locally sourced and deposited, because older wood transported by a river is not likely to be preserved after erosion and redeposition. From the 48 cores along transects BNGB and BNGC, 29 wood samples, 2 grass samples, and 1 organic sediment sample were analyzed for radiocarbon age dating at the National Ocean Sciences AMS dating facility at Woods Hole Oceanographic Institution. All ages are reported in calibrated, sidereal years (cal yr BP), with calibrations performed using Calib 6.0 software (Stuiver and Reimer, 1993).

v. Sediment geochemistry

Bulk sediment geochemistry was measured using a Thermo Scientific Niton handheld X-ray fluorescence (XRF) analyzer. Major elements concentrations generally reflect grain-size variations in the relative proportion of SiO_2 and Al_2O_3. However, strontium concentrations in the GBMD have been shown to be a useful provenance indicator for the different fluvial systems delivering sediment to the GBMD (Singh et al., 2006; Garzanti et al., 2010; Pickering at al., 2013). Strontium primarily substitutes for calcium in mineral lattices due to their similar charge and ionic radius, with plagioclase feldspar and epidote being the principal Sr-bearing minerals in the GB delta (Garzanti et al.,2010). For Holocene sediments, it has been shown that difference in strontium concentrations between the GBMD fluvial sources is considerably greater than the variation caused by weathering or hydraulic sorting (Goodbred et al., *in press*). 150 samples were initially prepared for XRF analysis by combusting at 650°C for 72 hours, leaching in 15% acetic acid to remove carbonates, and then powdering in a shatterbox. However, a comparison was made between strontium concentrations in samples prepared using this time-consuming approach versus samples that were only dried, and it was determined that the difference in strontium concentrations was ±10%, or nearly within the range of analytical error (fig. 8). In this case the remaining samples were dried only, allowing a total of 675 samples to be analyzed from the two transects.
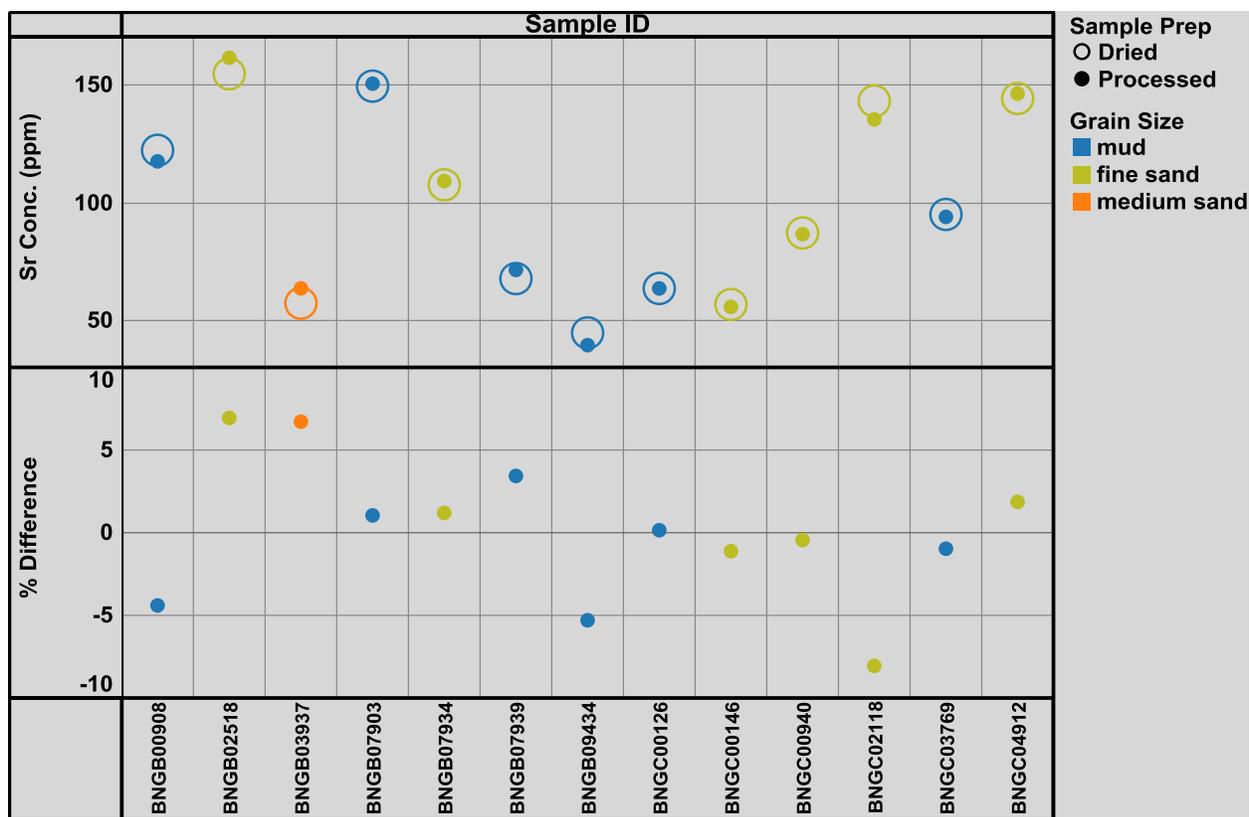
Figure 8. Sample preparation comparison. Strontium concentration between samples that were fully prepared through combustion, carbonate leaching, and powdering and samples that were dried only.

vi. Magnetic susceptibility

The magnetic susceptibility (MS) was measured for all 2051 samples using a Bartington Magnetic Susceptibility meter. MS is measured as the relative magnitude of temporary magnetization that results from exposure to an induced magnetic field (Kimbrough et al.; 1997). Samples with a greater amount of heavy magnetic minerals such as magnetite, illmenite, and hematite will have greater MS values (Jones and Beavers, 1964). MS of sediment samples reflects mineralogical character of the source material and has been used in other studies as a provenance indicator where there have been multiple sediment sources (Glass et al., 1964; Grimley et al., 1998; Kimbrough et al., 1997; Zhang et al.; 2008; Maher et al.; 2009).

Strontium concentration and MS reflect bulk sediment mineralogy but are controlled by different mineral suites, thus providing unique lithologic discriminators. Strontium concentrations reflect the abundance of calcium-bearing minerals, including plagioclase, epidote, and the phyllosilicates, none of

17

which have magnetic response (Fairbridge, 1972). Grain size does influence both Sr concentration and

MS (Garzanti et al., 2010), but a comparison of these attributes for mud, fine sand, and medium sand

sediment populations demonstrate that it is not a principal control (Fig. 5) (Pickering et al.; 2013).

Chapter III

Results

A. Sediment lithology introduction

Grain size, color, geochemistry, and plasticity were used to define sediment lithology and
determine depositional environment and provenance. The late Pleistocene lowstand surface is
recognized as a weathering horizon of variable thickness ranging from several meters in low-permeability
muds to tens of meters in well-drained sands. This paleosol surface is readily identified by its orange to
brown oxidation state and the low plasticity of muds (Figs. 11-13, 16; Goodbred and Kuehl, 2000; Pate et
al., 2009; Pickering et al., 2013). Radiocarbon dates further constrain the timing of deposition of different
lithologic units.

B. Grain size

    i. Dominant size distributions

Among the full dataset, there are two dominant grain size distributions that include silt-dominated
muds (>80% silt; <20% clay or sand) and clean sands (>80% sand, <20% silt) (fig. 9). A third,
comparatively infrequent size distribution includes equal parts of silt and fine sand. Of 171 samples , only
~3% have a clay fraction of >20%, reflecting the generally coarser silt and sand dominated sediment load
of the rivers. Silt and sand sized particles are the dominant grain sizes in the Meghna valley with ~46%
of samples having a silt fraction of >50% and ~54% with a sand fraction >50%. Sand size distributions
show a division between fine-sand dominated samples and medium-coarse sand samples, with this
division occurring due to fine sand preservation in the silt-dominated mud samples (fig. 10).
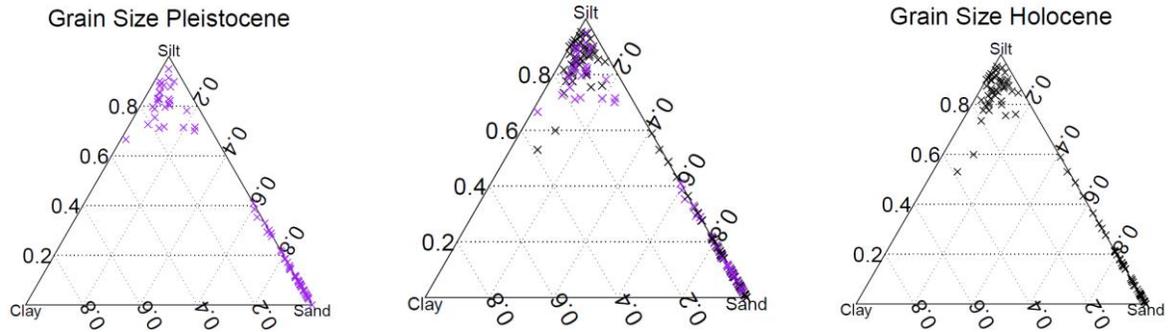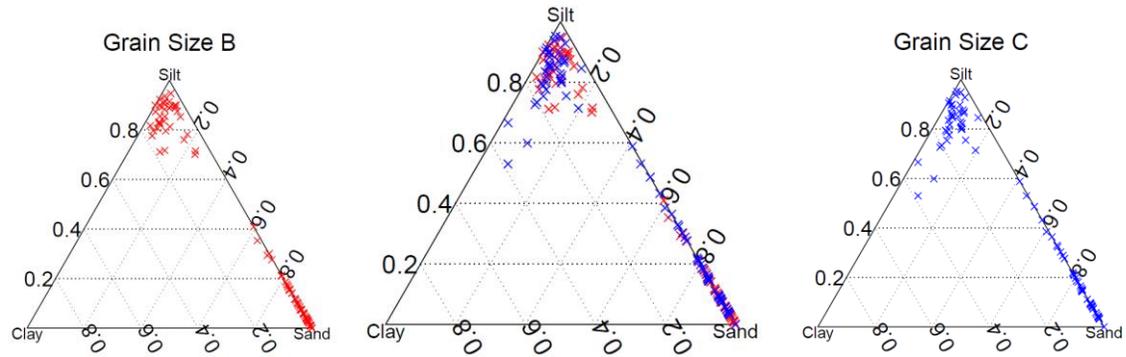
Figure 9. Clay-silt-sand plots. Grain size plots of particle analyzer grain size data for select samples in BNGB and BNGC with a Pleistocene to Holocene comparison in the top plots and a BNGB to BNGC comparison in the lower plots.
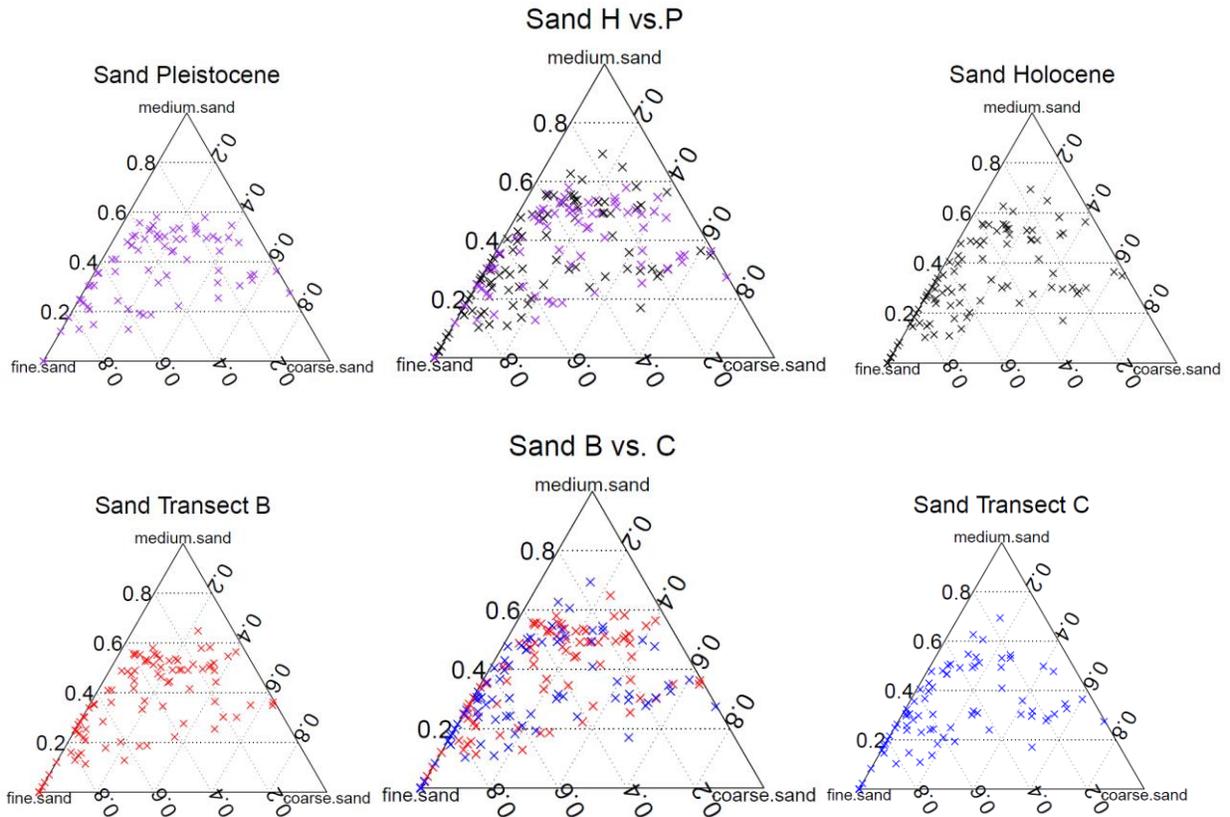
Figure 10. Fine-Medium-Coarse sand plots. Grain size plots of particle analyzer grain size of sand fraction same select samples in figure 6 in BNGB and BNGC with a Pleistocene to Holocene comparison in the top plots and a BNGB to BNGC comparison in the lower plots.

ii.   Fine sediment preservation in the Holocene and at valley margins

There is a considerable amount of fine grained sediment preserved in BNGB and BNGC in comparison to BNGA at the upstream entrance to Sylhet basin (Pickering et al., 2013). Particularly the Holocene section of the Meghna valley is notable for its preservation of finer grained sediments in its abundance of silts and fine sands which are certainly lacking in the upstream Holocene deposits of BNGA (fig. 9, 10). In BNGA, Holocene mud deposits only occur in the upper 10 m of the stratigraphy as flood plain deposits and valley edge deposits alongside fluvial-valley-bounding features. For BNGB and BNGC, the size and location of these finer units falls into three categories: thick mud units of 10-30 m at

the valley edges by Madhupur terrace and the Indo-Burman fold belt, thin mud units of less than 5 m occurring locally within the thick sand bodies of >20 m in the main valley, and a Holocene base mud unit, 25-30 m thick, that extends 40 km across the central valley (fig. 11).

iii. B/C Holocene comparison - downstream fining

For the Holocene, the overall grain size of BNGB is coarser than for BNGC despite being only 25-60 km upstream from BNGC (fig. 9, 10). There are a few ways that this difference appears in the stratigraphy: (1) in the large amount of mud preserved in thick 10-30 m units in the Holocene valley in BNGC and (2) in the difference in grain size in sand units between BNGB and BNGC. The wide valley in BNGC is primarily filled with mud, up to 40 m thick, in the lower Holocene stratigraphy, accounting for fully 50% of total Holocene stratigraphy comprising mud. The same thick, lower Holocene mud is found along BNGB,, but the narrower valleys at that location has led to reworking and erosion of these muds, which are preserved in relatively thinner unit in only a few cores (fig. 11). For both transects, the thickness of muds >10 m, the regular presence of wood fragments, and lack of gastropod shells that are regularly preserved in lower estuarine deposits suggest that these thick mud units are flood basin deposits like those described from central Sylhet basin throughout the Holocene (Goodbred and Kuehl, 2000; Goodbred et al., 2003). The sand found in BNGB in the upper 30-40 m is mostly medium to coarse sand with a volume weighted mean of ~300 μm, whereas the sand in the upper stratigraphy of BNGC is primarily fine sand with a volume weighted mean of ~225μm. This decrease in sand size over 100 km or less between BNGB and BNGC is a consequence of the complete extraction of coarser size fractions by this point along the channel flow path, where coarse fractions are preferentially extracted until they decline to zero (Paola and Martin, 2012). The differences in channel width could also be a factor in extraction of courser sands in the narrower valleys in BNGB and finer sand deposition in the wider valley in BNGC.
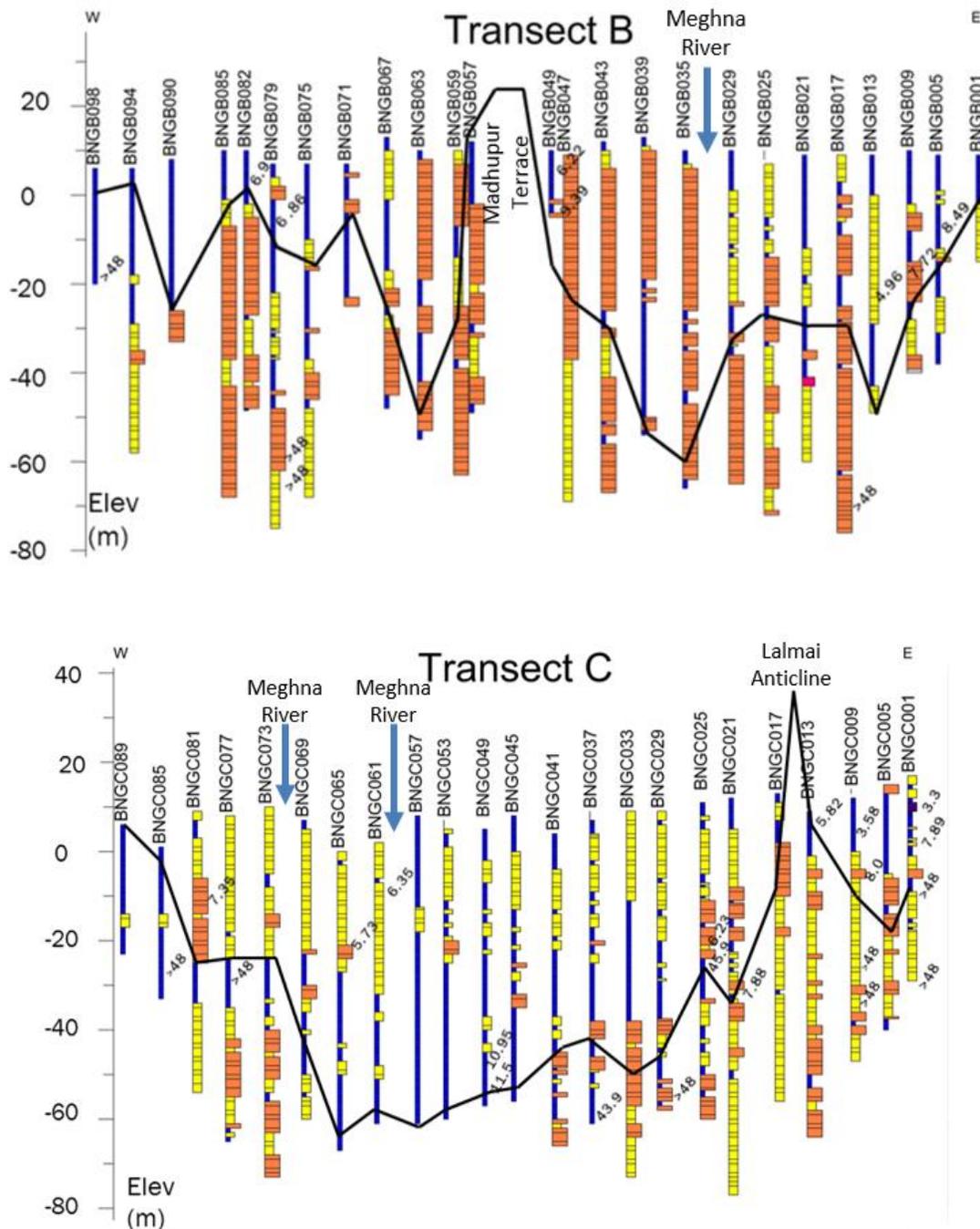
Figure 11. Cross sections displaying dominant grain sizes. Cross sections of BNGB and BNGC displaying grain sizes from three categories. Blue = mud, yellow = sand, and orange = medium to coarse sand. The Holocene-Pleistocene boundary is marked in black and age dates are marked in kyr B.P. on the cores. V.E = 500. The current Meghna channel is marked by the blue arrows.

23

C. Geochemistry

      i. Strontium ranges

Bulk-sediment strontium (Sr) concentrations in the Meghna valley range from 11- 209 ppm (fig. 12). These Sr concentrations are comparable to previous studies for the GBMD (Singh and France-Lanord, 2002, Pickering et al, 2013; Goodbred et al., *in press*). Based on the two known fluvial inputs of sediment into the Meghna valley from the Brahmaputra and the BSK rivers, Sr concentrations obtained in this study are divided into four groups: high (140 or greater ppm), mid (90 to 140 ppm), low (60 to 90 ppm), and very low (less than 60 ppm). These designations were made based on known values for the BSK rivers found in cores in Sylhet basin (Goodbred et al., *in press*), Brahmaputra River (Singh and France-Lanord, 2002, Pickering et al, 2013; Goodbred et al., *in press*), and local upland-stream sources (Pickering et al, 2013). The lowest Sr concentrations <60 ppm correspond to local sediment sources originating from the small streams draining weathered Neogene delta deposits in the Indo-Burman fold belt (fig. 4). Deposits of these sediments are found along the valley margins, primarily of Pleistocene age but also locally within the Holocene. Sediment having 60-90 ppm Sr is associated with the BSK river system (Goodbred et al., *in press*) and comprise most of the late Pleistocene deposits of the Meghna valley. In the Holocene, though, such BSK deposits are more restricted in their distribution, being found primarily along the eastern portion of the valley and in units only several meters thick. Instead most of the Holocene stratigraphy comprises deposits having >140 ppm Sr, corresponding with deposition by the Brahmaputra (Singh and France-Lanord, 2002; Pickering et al., 2013). Intermediate Sr concentrations from 90-140 ppm have no known source, initially suggesting that such sediments reflect mixing between the Brahmaputra and BSK rivers when both are occupying the Syhet basin.
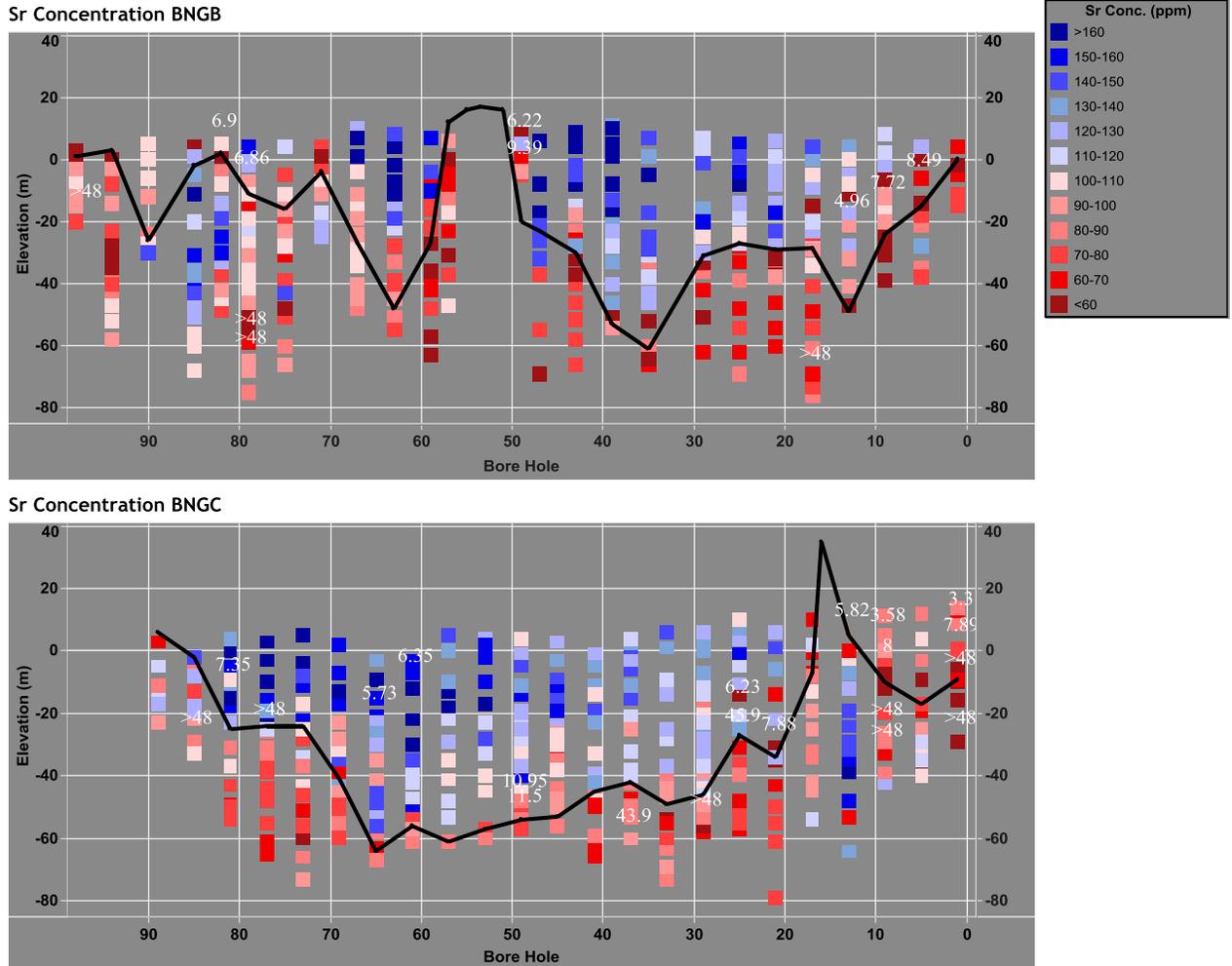
Figure 12. Intensity plot cross sections of strontium concentrations. Radiocarbon dates in kyr BP and Holocene Pleistocene boundary drawn in black.

ii.   Magnetic susceptibility ranges

Based on the association of particular MS ranges with specific lithologic units discerned by grain size (fig. 11,13), MS groupings are identified as high ($>50 \times 10^{-6}$), mid (20-50×10^{-6}), and low ($< 20 \times 10^{-6}$). The Brahmaputra's sediment mineralogy has higher MS of $>50 \times 10^{-6}$ than sediment from the BSK rivers or the valley margin sources with MS $< 20 \times 10^{-6}$. Thus, high MS values generally correspond to Brahmaputra sediment and low to BSK or local sources, with mid ranges being considered a mixed source. High MS sediments in BNGB and BNGC are found in the Holocene valley and a few Pleistocene

sites in sand bodies of up to 50 m thickness and muds of up to 5 m thickness. Mid MS sediments are also

prevalent in the Holocene valley corresponding to the thick mud unit at the valley base and sand units up

to 15 m in thickness. Low MS sediment is found at the valley margins and prevalent in the Pleistocene

sediments corresponding to sediment not from the Brahmaputra River thus local and BSK rivers in origin.

These patterns also match those of MS values for sediments upstream along BNGA and the Old

Brahmaputra valley, where deposits within the main valley system have high MS corresponding with

Brahmaputra sediments and lower MS sediment is found along the valley margins that are sourced from

local streams (Pickering et al., 2013).
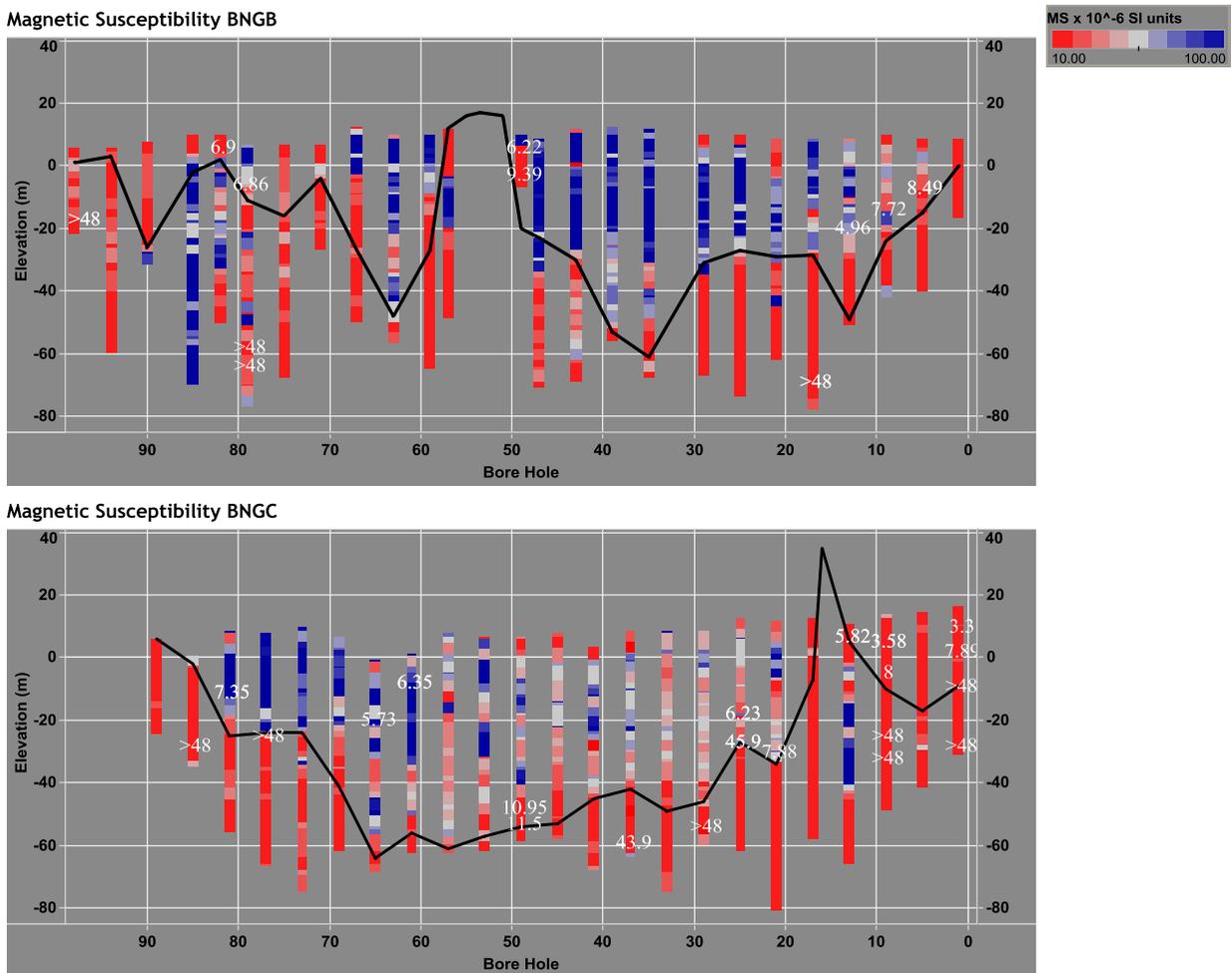
Figure 13. Intensity plot cross sections of magnetic susceptibility.   Radiocarbon dates in kyr BP and Holocene Pleistocene boundary drawn in black.

Sr concentrations and MS values correlate with a regression coefficient of 0.54 and has statistical significance based on 648 samples, which includes the full range of sediment age, grain size, and river source (table 1). Furthermore a plot of these data based on sediment size classifications (fig. 14) demonstrate the same general relationship, indicating that grain size is not the principal control on MS. Rather, Sr concentration and MS are independent variables, controlled by plagioclase/epidote and ferromagnesian/ferro-oxic minerals, respectively. Thus Sr and MS are primarily controlled by source mineralogy and weathering state, characters that can be considered tractable indicators of sediment provenance. Taken together with grain size distributions, these sediment attributes can aid in defining lithofacies and their stratigraphic and spatial distribution in the Meghna valley.

Table 1. Strontium concentration and magnetic susceptibility correlation data

Grain Size	R-squared	Coefficient	Intercept	n	P-value
All	0.54	23.09	22.58	648	< 0.0001
Mud	0.42	23.48	22.12	258	< 0.0001
Fine Sand	0.68	24.86	21.77	206	< 0.0001
Medium Sand	0.41	20.08	25.59	184	< 0.0001
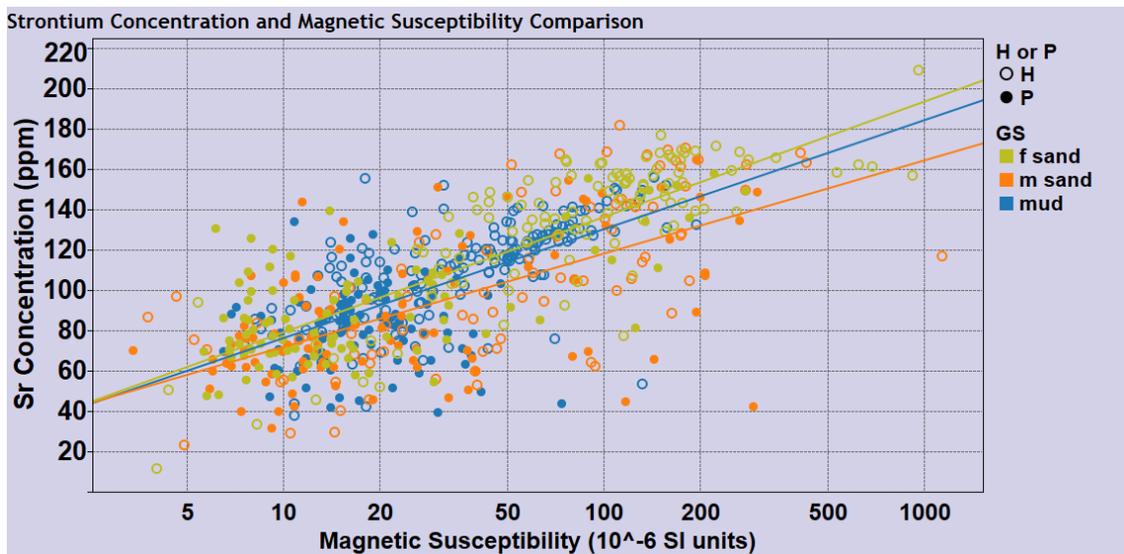
Figure 14. Strontium concentration compared to magnetic susceptibility values from all samples from BNGB and BNGC.

D. Radiocarbon

Nineteen of 32 radiocarbon samples from the Meghna valley yielded Holocene ages from 11.5 to 3 kyr BP (table 2). The Holocene dates have a dominant mode between ~9 to 5 kyr BP, with smaller modes ~11.5 to 11 kyr BP and ~3.5 to 3 kyr BP (fig. 15a). Holocene radiocarbon samples were associated with a variety of lithologies: eight from local alluvial muds, four from channel bar sands, three from braidbelt sands, two overbank muds, and two basinal muds (fig. 15). Overall, radiocarbon datable material was recovered at shallower depths within mud units that were deposited as shallow overbank and slackwater environments along the valley margins, as compared with sand deposition that occurred within channels that may be 10-15 m lower than floodplain elevations. As well, a greater amount of organic material is preserved on the valley margins, most likely reflecting more frequent reworking of central valley sands by channel migration, not allowing organic matter to be deposited or preserved.

Within the Holocene valley, the two basinal mud samples from BNGC049 situated at the center of the Meghna paleovalley yield the oldest Holocene ages of 10.9 and 11.5 kyr BP, placing sediment deposition at this time just after the end of the Younger Dryas cold phase (Broecker et al., 2010). The dominant mode of ~9-5 kyr BP is distributed both in valley edge and channel deposits corresponding to the same timing of major deposition in the Old Brahmaputra course upstream (Pickering et al., 2013). In addition to Holocene radiocarbon ages, thirteen samples yielded largely radiocarbon-dead Pleistocene ages ranging >48 to 43.9 kyr BP. Pleistocene radiocarbon samples showed less distribution lithologically with eight from channel bar sands, three from terrace muds, one from overbank muds and one from basinal muds.

Table 2. Summary of radiocarbon results

| Lab ID	Sample ID	Transect	Site	Depth	Grain Size	Material	Lithology	d¹³C	¹⁴C age BP		cal yr BP	2σ upper	2σ lower
OS-99280	BNGB00517	B	5	17	mud	wood	local alluvial mud	-27.7	7710	±90	**8492**	8415	8582
OS-99281	BNGB00925	B	9	25	mud	wood	local alluvial mud	-28.7	6890	±80	**7722**	7656	7830
OS-99282	BNGB01330	B	13	30	f. sand	wood	channel-levee sand	-28.1	4400	±60	**4962**	4866	5211
OS-99283	BNGB01779	B	17	79	m. sand	grass	channel-levee sand	-14.7	>48000	—	**>48000**	—	—
OS-99314	BNGB04905	B	49	5	mud	wood	local alluvial mud	-28.2	5390	±60	**6217**	6026	6284
OS-99391	BNGB04914	B	49	14	mud	wood	local alluvial mud	-30.7	8370	±110	**9392**	9255	9519
OS-99390	BNGB07914	B	79	14	mud	wood	overbank mud	-27.1	6020	±80	**6863**	6747	6959
OS-99315	BNGB07966	B	79	66	m. sand	wood	channel-levee sand	-29.1	>48000	—	**>48000**	—	—
OS-99316	BNGB07972	B	79	72	f. sand	wood	channel-levee sand	-29.7	>48000	—	**>48000**	—	—
OS-99317	BNGB08205	B	82	5	mud	wood	overbank mud	-30.2	6050	±100	**6903**	6748	7151
OS-99318	BNGB09824	B	98	24	mud	wood	terrace mud	-30.3	>48000	—	**>48000**	—	—
OS-99319	BNGC00108	C	1	8	mud	wood	local alluvial mud	-27.9	3070	±50	**3298**	3218	3360
OS-99320	BNGC00116	C	1	16	mud	wood	local alluvial mud	-27.0	7060	±90	**7892**	7794	7966
OS-99321	BNGC00127	C	1	27	f. sand	wood	channel-levee sand	-27.1	>48000	—	**>48000**	—	—
OS-99322	BNGC00146	C	1	46	f. sand	wood	channel-levee sand	-28.7	>48000	—	**>48000**	—	—
OS-99323	BNGC00910	C	9	10	mud	wood	local alluvial mud	-28.1	3340	±60	**3577**	3477	3677
OS-99324	BNGC00920	C	9	20	m. sand	wood	channel-levee sand	-28.3	7190	±80	**7999**	7938	8154
OS-99392	BNGC00940	C	9	40	f. sand	wood	channel-levee sand	-28.3	>48000	—	**>48000**	—	—
OS-99393	BNGC00947	C	9	47	f. sand	wood	channel-levee sand	-29.8	>48000	—	**>48000**	—	—
OS-99394	BNGC01306	C	13	5.5	mud	wood	local alluvial mud	-27.2	5110	±60	**5817**	5750	5923
OS-99395	BNGC02143	C	21	43	m. sand	wood	channel-levee sand	-29.5	7040	±100	**7877**	7757	7965
OS-99396	BNGC02532	C	25	32	m. sand	wood	channel-levee sand	-27.8	5410	±70	**6233**	6031	6293
OS-99397	BNGC02541	C	25	41	mud	wood	overbank mud	-29.6	43500	±9400	**45902**	39359	50000
OS-99455	BNGC02964	C	29	64	m. sand	wood	channel-levee sand	-28.5	>48000	—	**>48000**	—	—
OS-99456	BNGC03769	C	37	69	mud	wood	basinal mud	-29.0	40100	±7600	**43924**	37789	50000
OS-99452	BNGC04956	C	49	56	mud	wood	basinal mud	-29.8	9570	±130	**10929**	10708	11156
OS-99453	BNGC04961	C	49	61	mud	grass	basinal mud	-15.1	10000	±140	**11494**	11245	11767
OS-99454	BNGC06111	C	61	11	f. sand	wood	braidbelt sand	-29.1	5550	±70	**6346**	6292	6402
OS-99457	BNGC06521	C	65	21	f. sand	wood	braidbelt sand	-31.8	5000	±70	**5728**	5645	5891
OS-100344	BNGC07734	C	77	34	mud	wood	terrace mud	-29.5	>48000	—	**>48000**	—	—
OS-99458	BNGC08121	C	81	21	m. sand	wood	braidbelt sand	-28.3	6420	±110	**7351**	7258	7429
OS-99398	BNGC08530	C	85	30	mud	sediment (TOC)	terrace mud	-27.6	>48000	—	**>48000**	—	—

29

a)

b)
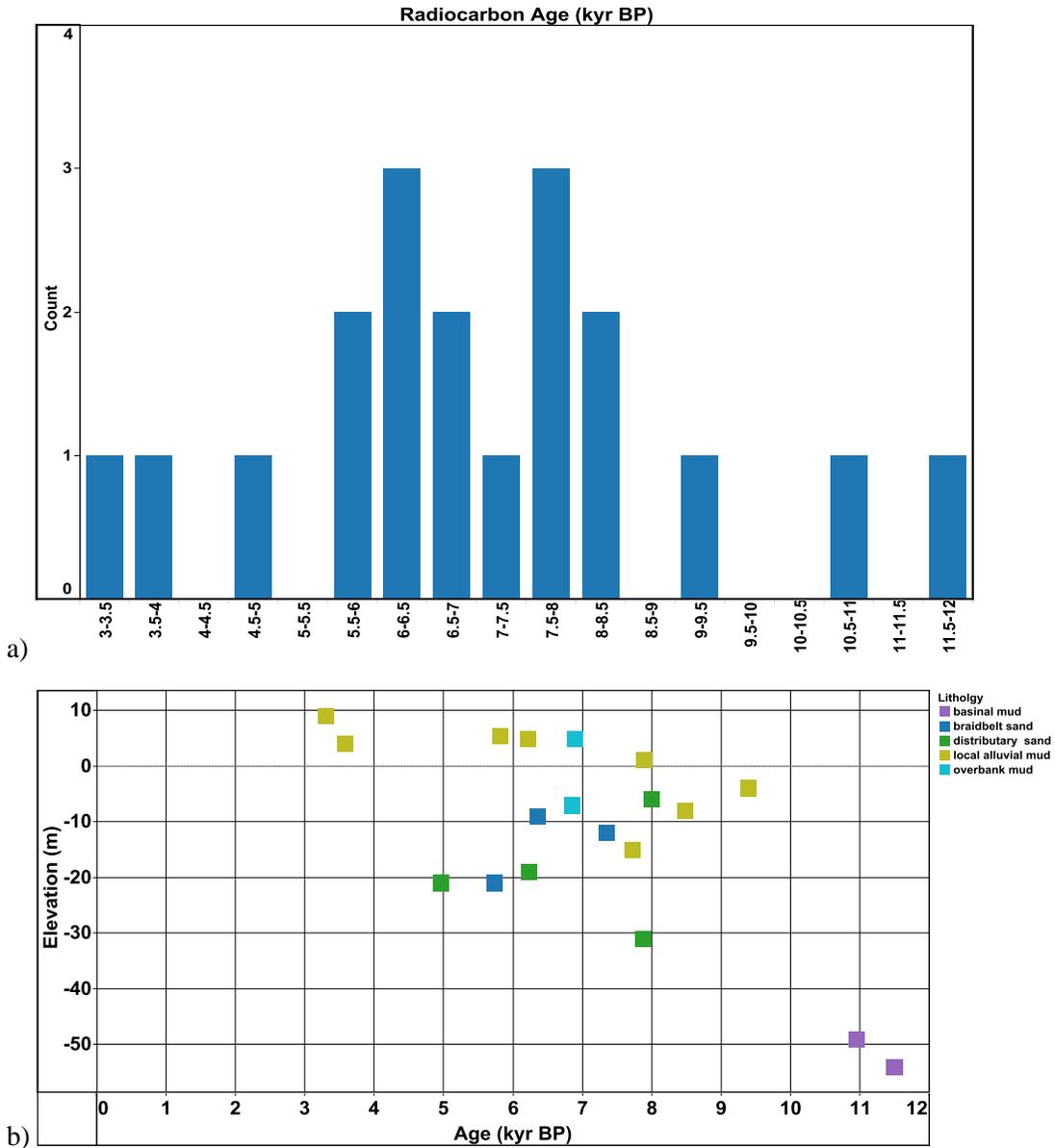
Figure 15. Holocene ages of radiocarbon samples. The top plot is a histogram of Holocene dates. Most ages are from 9 to 5 kyr BP with only several ages from the early (~11.5 to 11 kyr BP) and late (~3 to 3.5 kyr BP). The bottom plot is of Holocene dates versus their depth colored according to the lithology of the sediment of the sample.

E.   Sedimentary facies

   i.   Basinal muds

Basinal muds are thick units 10-40 m thick that reflect slackwater sediment deposition in the absence of a nearby major fluvial channel and associated sand input. Sand-dominated lithologies dominate other portions of the GBMD, and thus the presence of thick mud units in the sedimentary record indicates the lack of a major fluvial sand source and absence of the principal fluvial channels from the Meghna River valley. Such muds are prevalent in the wide valley crossed in transect BNGC (C029-069) but are only locally preserved in the narrower valleys in BNGB (B013, B039, B063) (fig. 11). The earliest Holocene deposits found in the Meghna valley along transects BNGB and BNGC are basinal muds that date 11.5 kyr BP in core C049 (fig. 11). These muds are initially derived from the BSK river system but show a transition to mixed, Brahmaputra-influenced muds early in the Holocene prior to the deposition of any Brahmaputra channel sands. These early Holocene muds can be correlated with basinal muds described from the central Sylhet based on their similar age and geochemical character (Goodbred and Kuehl, 2000; Goodbred et al., *in press*).

   ii.   Overbank Muds

Throughout the GBMD, mud deposition associated with overbank flow of channels constructs fine-grained floodplain deposits up to several meters thick (Goodbred and Kuehl, 2000), and these are widely recognized within the Meghna valley. Examples of these deposits are provided by the widespread cap of floodplain muds that are preserved in the surficial Meghna valley stratigraphy, as well as the thin mud layers separating braidbelt and channel-levee sands within the middle and lower Holocene stratigraphy (fig. 11). The overbank muds are distinguished from basinal muds in being comparatively thin (<10 m) and separated by sand layers that are sourced by nearby fluvial channels. Within the main Holocene valleys, however, overbank muds are not well preserved due to lateral channel migration and

sediment reworking, which is similar to the processes and stratigraphy described for the Holocene valley along the upper Old Brahmaputra channel (i.e., transect BNGA; Pickering et al., 2013).

<p style="text-align:center">iii.   Channel-levee sands</p>

In the Meghna valley, sand deposits range in thickness from a few meters to tens of meters. The thinner sand deposits (<10 m) are much smaller than those developed by the main Brahmaputra braidbelt (e.g., Pickering et al., 2013) and instead represent channel levee sands formed by smaller fluvial systems or a distributary of the Brahmaputra. Because sand provenance can be determined from the sediment geochemistry, we note that the thin channel-levee sands in the deepest Holocene valley deposits (cores B035-039, B063, C029-037) are sourced by the BSK fluvial system, having with low Sr concentrations from 60-90 ppm and MS < 20 x 10^{-6} (fig 11). The lateral extent of these deposits is not more than several cores spanning no more than ~10 km, further supporting that these deposits do not represent the full Brahmaputra braidbelt system.   Only lower Sr and MS channel-levee sands are present in the earliest Holocene sand deposits indicating that the BSK river system was the dominant fluvial source at the beginning of the Holocene in the Meghna valley (fig. 14).

Locally there is also 3-5 m of Brahmaputra sourced sand with high Sr and MS values at ~ 50 m depth near the base of the lowstand valley in cores C041-049 and C061-069 (fig. 16), which date to the early Holocene based on several nearby radiocarbon ages ~10.5-11.5 ka, and given their relatively small dimensions were sourced by a distributary of the Brahmaputra. The 3-5 m thickness of these sand units also suggests a short delivery period $\leq 10^2$ yrs based on radiocarbon dating from this and previous studies (Goodbred and Kuehl, 2000). The inference of a short early-Holocene occupation of the Sylhet basin and Meghna valley by the Brahmaputra, or one of its distributaries, is consistent with findings from the main avulsion node and the central Sylhet basin, which both record local inputs of Brahmaputra sands sometime between 9.5-11.0 ka (Goodbred and Kuehl, 2000, Pickering et al., 2013, Goodbred et al., *in press*).

Channel-levee sands are also the principal facies preserved in the late Pleistocene deposits below the valley floor (fig. 14), comprising amalgamated channel-levee sands 20-30 m thick with occasional overbank muds of only a few meters, (fig. 16). This amalgamation of stacked channel-sand bodies accounts for the relative thickness of these deposits formed by the comparatively small BSK fluvial system, given that modern BSK discharge is only ~10% that of the Brahmaputra.

iv.   Braidbelt Sands

Braidbelt sands are identified as being 10-30 m thick and have lateral dimensions > 10 km (Goodbred and Kuehl, 2000; Pickering et al., 2013) and deposited in fluvial valleys by large-sediment laden rivers that deposit sand within the channel in the form of bars. In the Meghna valley, there is a large body of sand 20-30 m thick and ~40 km wide having high to intermediate Sr and MS values, which is found along BNGC in cores C021-C081 and in the two subvalleys of BNGB in cores B013-B067 (fig. 14). The highest Sr and MS values that are considered to represent end-member Brahmaputra sediments are found in the westernmost portion of the valleys, while intermediate Sr and MS values reflecting a mix of Brahmaputra, BSK, and local sediments are found in the central and eastern portions of the valleys. Radiocarbon dates constrain this Brahmaputra-dominated braidbelt deposit to ~7.5-5 kyr BP. This deposit, constructed over a period of ~2.5 kyr while the Brahmaputra occupied its Sylhet basin course and the Meghna valley, comprises nearly the entire upper 30 m of valley stratigraphy and is marked by sediment having either an end-member Brahmaputra or mixed, Brahmaputra-influenced provenance. Development of these sand-dominated units in the Meghna valley correlates with deposits of the same scale and time of deposition in the upper Sylhet basin (Pickering et al., 2013).

v.   Relating sediment facies to sediment provenance

Measured attributes of sediment infilling the Meghna valley help to define distinct lithologies that are separated into provenance groups (table 3, fig. 16). These provenance groups include (*i*) Brahmaputra-derived sediments characterized by high Sr and high MS values, (*ii*) BSK-sourced sediments having low

33

Sr and low MS, (*iii*) mixed-source sediments (i.e., Brahmaputra plus BSK or local sources) with mid Sr and mid MS, (*iv*) local alluvium with very low Sr and low MS, and (*v*) Pleistocene-age deposits having mid to low Sr values and mid to low MS that are of mixed local and fluvial sediment (table 3). The major Brahmaputra braidbelt deposit in the Meghna Holocene valley is a large sand package of up to 30 m thickness. This sand package accounts for the upper part of Holocene infill around the eastern part of Madhupur Terrace in the center of BNGB and the western side of the main valley in BNGC, and mixed Brahmaputra and BSK sediment deposits account for most of the other Holocene valley infill in the upper stratigraphy. Brahmaputra sediment is found in smaller meter-scale channel-levee sand deposits earlier in the Holocene in BNGC, which is of note because this scale of deposit is significantly smaller than other Brahmaputra braidbelt deposits, suggesting a relatively short occupation period ($<10^2$ yrs) by a distributary of the Brahmaputra (fig. 5). BSK fluvial deposits are not prevalent in the Holocene stratigraphy except at the eastern margin of the Meghna valley and overlying the Holocene-Pleistocene boundary. However, Pleistocene-age deposits are dominated by sediment from the smaller BSK rivers and locally sourced sediment from the valley edges (table 3, fig 16), indicating no influence of the Brahmaputra during the last sea-level lowstand.

In the Meghna valley, only a few cores have high Sr and high MS Brahmaputra deposits in the Pleistocene-age sediment, making its occurrence in the late Pleistocene fairly rare. It could be argued that the Pleistocene deposits in the Meghna valley have been weathered and thus have lower Sr and MS, but this does not appear to be the case when compared with results from Pleistocene deposits of BNGA (fig. 5), which have high Sr and MS values and are almost entirely of Brahmaputra-origin (Pickering, et al., 2013). So instead of a weathering signature, the Sr and MS are showing a source signal that allow for channel occupation history over time to be determined.

34
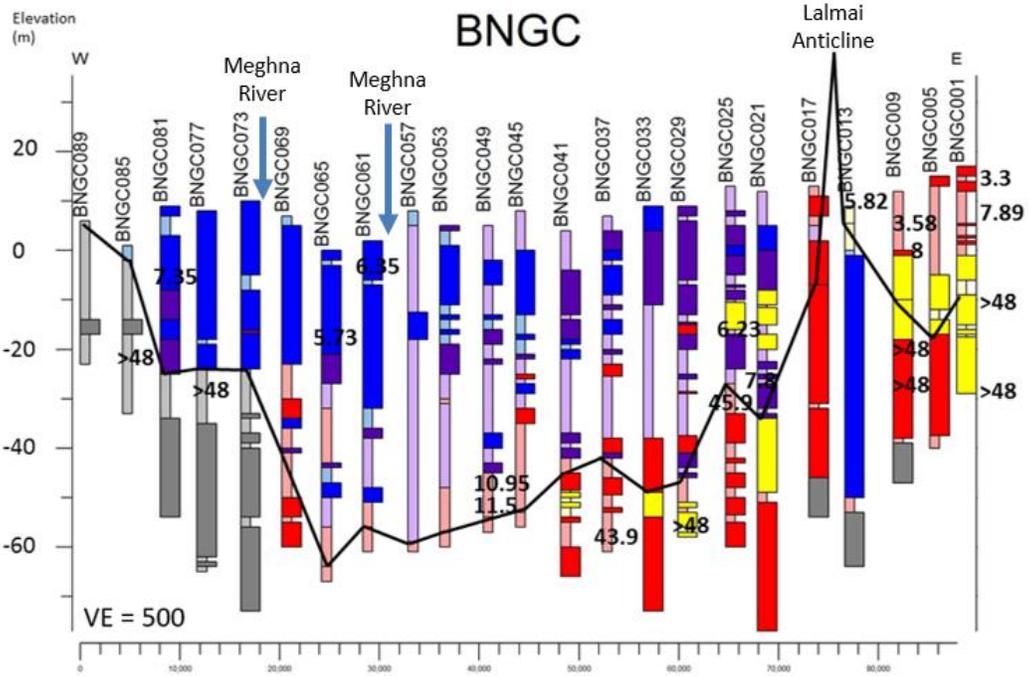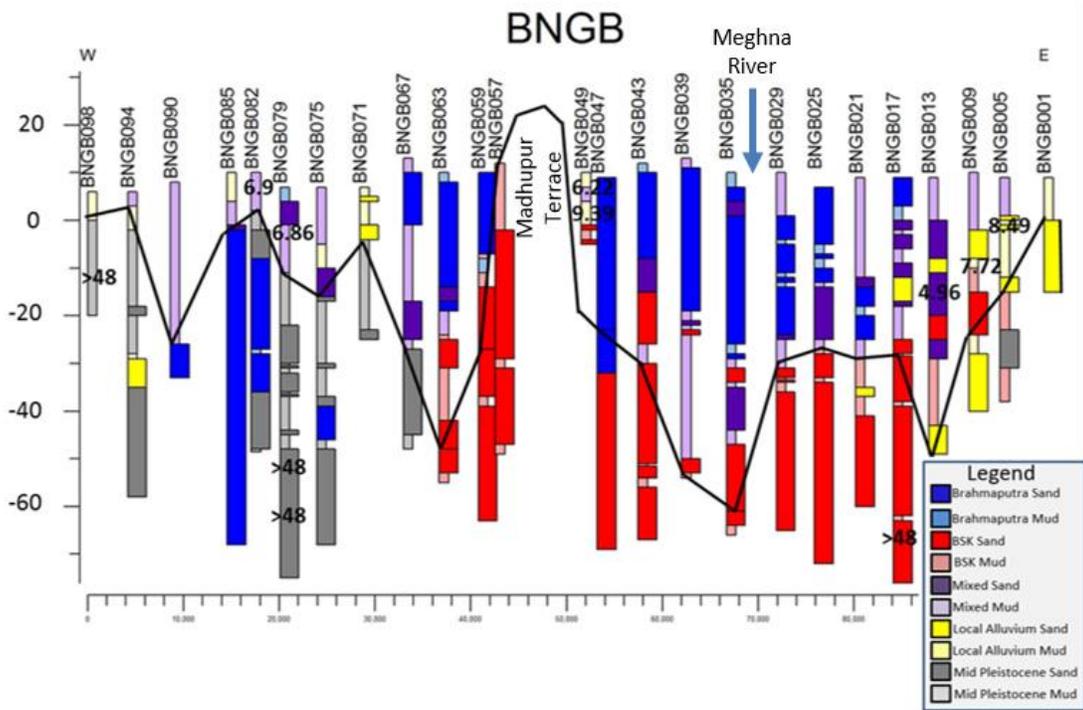
Figure 16. Stratigraphic cross sections. Radiocarbon dates in kyr BP and Holocene-Pleistocene boundary drawn in black.

Table 3. Stratigraphic provenance and facies

Provenance	Sr Conc. (ppm)	Mag Susc.(10^{-6} SI)	Sand facies, thickness, and characteristics	Mud facies, thickness, and characteristics	Holocene locations	Pleistocene locations	Interpretation
Brahmaputra	>140	>50	Almost entirely-braidbelt sands Early Holocene-channel-levee or distributary sands Holocene: gray, 30 m typical Pleistocene: oxidized 30-60 m	Overbank muds Holocene: gray, several meters in thickness, interbedded with large sand packages Rare in Pleistocene	Upper 40 m of main channel valleys--BNGB017-047, BNGB059-067, and BNGC041-081	Only found in a few cores: B047, B075, B082-90, C013	From Brahmaputra when it occupies its eastern Old Brahmaputra course
Mixed	90-140	20-50	Braidbelt sands Gray, 10-20 m	Gray, large basinal muds up to 40 m and overbank mud deposits of several meters	Associated with main channel valleys both in channel fill and basin fill--BNGB005-013 and BNGC017-41	N/A	BSK sediment mixed with Brahmaputra sediment, local influence is possible also
Barak-Surma-Kushiara	60-90	<20	channel-levee sands Holocene: gray, 10-15 m and smaller several meter deposits, Pleistocene: gray, 30-40 m	Basinal and overbank muds Holocene: gray, up to 20 m, Pleistocene: gray, several meters	First deposition in the Holocene in main valleys and east of Lalmai anticline (C001-C013)	Below Holocene valley	BSK rivers input of sediment without the Brahmaputra with possible local input
Local alluvium	<60	<20	Typically tan to brown and quartz rich, up to 15 m	Gray to reddish brown, up to 10 m	Valley edges	Valley edges	Locally sourced sediment from valley edges, from Madhupur terraces on the western side and the Indo-Burman fold belt to the east
Mid Sr Pleistocene (Mixed)	60-140	<50	Pleistocene: up to 30 m gray to reddish brown	Pleistocene: gray to reddish brown, several meters to 20 m		B005, B067-082, B090-98, C009-C017, C085, C089 and C073-C089	Mix of local with main channel sediment

Chapter IV

Discussion

A. Late Pleistocene evolution of the Meghna valley

i. Pleistocene channel dominance

The widespread sediments with low Sr concentration of 60-90 ppm and low MS values of $< 20 \times 10^{-6}$ below the Holocene boundary indicate that the BSK rivers were the dominant sediment source during the late Pleistocene. The abundance of BSK sediments and the lack of Brahmaputra sediments at this time indicate that Brahmaputra was not connected to Sylhet basin during the last glacial maximum and sea-level lowstand. Upstream of the Meghna valley, however, Brahmaputra sediments are well preserved across the Holocene-Pleistocene contact (Pickering et al.; 2013). In this Old Brahmaputra valley, the provenance is overwhelmingly Brahmaputra-sourced for Pleistocene and Holocene sediments, and only at the valley edges are there sediments derived from local sources off the Shillong Plateau (fig. 5). By contrast in the Meghna valley, the Holocene and Pleistocene sediments are sourced from different fluvial systems (fig. 16), with the BSK rivers the largest contributor of sediment to Sylhet Basin at the end of the Pleistocene. The difference in Pleistocene sediment sources for the upper and lower Sylhet basin suggest that the shallowest Pleistocene sediments along the Old Brahmaputra course are older than those along the Meghna valley and correlated with an earlier sea-level highstand (ie., pre MIS-2).

ii. Implications of Pleistocene Brahmaputra sediment

The Pleistocene section of core BNGC013 preserves an anomalous 50-m section of Brahmaputra braidbelt sands that are uncorrelated with the adjacent Pleistocene stratigraphy, which almost exclusively comprises local foldbelt or BSK-derived sediments (fig. 16). Most significantly, the presence of Brahmaputra sands in this one core at least confirm that the main braidbelt had traversed this area some time in the Pleistocene, but at some point became excluded from this course as reflected by the absence of latest Pleistocene Brahmaputra sands. The Pleistocene Brahmaputra sediments are uniquely associated

with the axis of the Lalmai anticline (figs. 6, 17) and, given their unique provenance and location, are presumed to have been preserved in association with growth of this structure. We suggest that absence of the Brahmaputra River beginning in the late Pleistocene was associated with advance of the Tripura thrust front and the onset of local folding and deformation that constructed the Lalmai anticline (fig. 16, 17)

iii.   Structural ties to Brahmaputra in the Pleistocene

Pleistocene Brahmaputra sediments are also locally preserved at sites B075 and B082-090 (red box in fig. 17), and are not correlated with the adjacent stratigraphy dominated by BSK deposits. Subtle topographic expressions (fig 4, 6) suggest that these isolated Brahmaputra channel sediments may also be associated with anticlinal structures as observe beneath the Lalmai anticline (fig 16). Such anticlines are known to develop at the west-propagating edge of deformation along the foldbelt accretionary wedge (Uddin and Lundberg, 2003; Sikder and Alam 2003). In this case the observed Brahmaputra sediments may have been uplifted within the growing anticlinal structures. At the core of the anticlines would be older sediment, which is apparent because the Brahmaputra sediment provenance contrasts markedly with the BSK sediments that widely define the latest Pleistocene valley fill (fig. 16). Further study is needed in the area of B085 to assess the buried structure and the extent to which the deformation front has extended into the Meghna valley. Also, the burial of structures that developed during the Pleistocene is plausible considering the large amount of Holocene sedimentation that has occurred during the post-glacial sea-level rise (Goodbred and Kuehl, 1999, 2000; Goodbred et al., 2003).
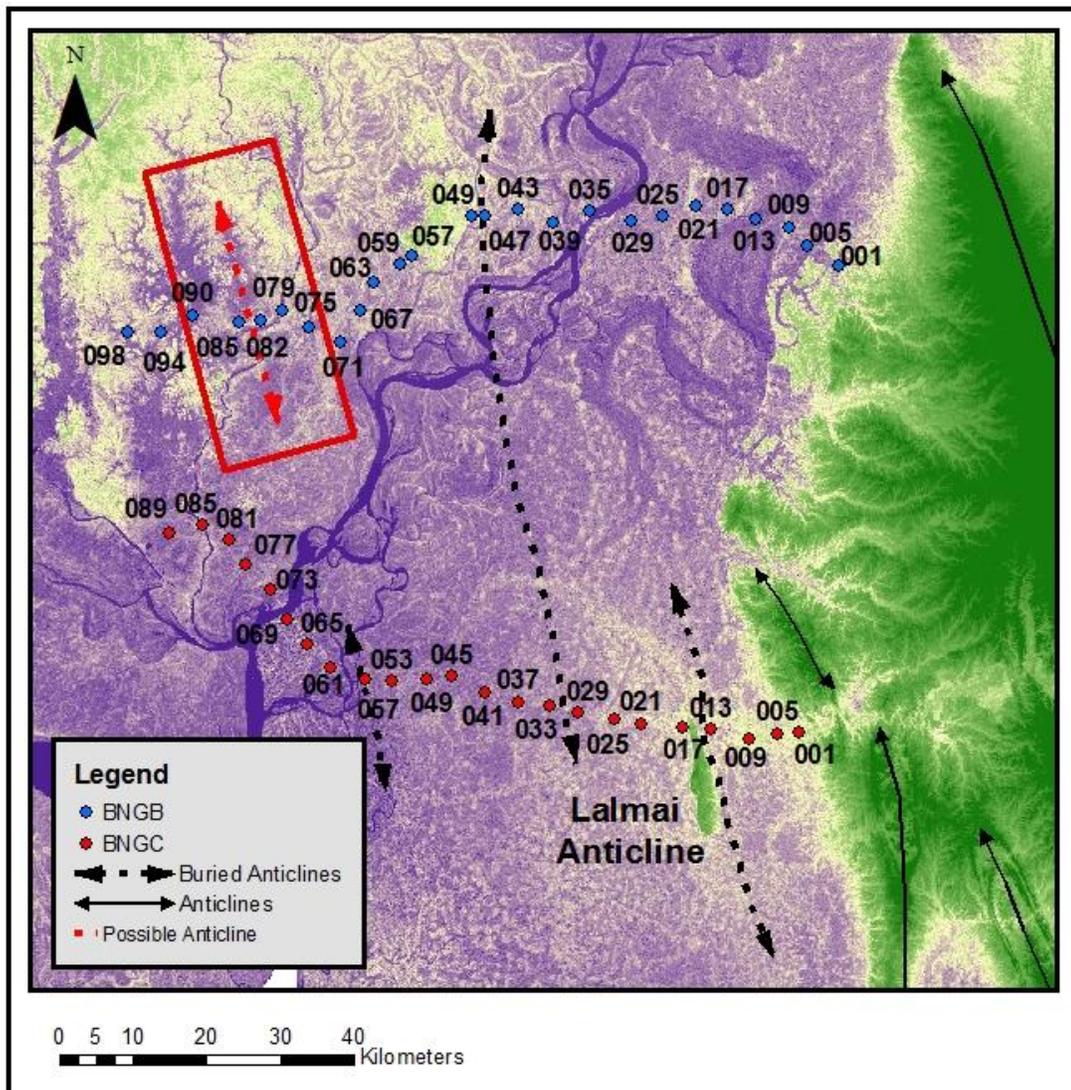
Figure 17. Anticline axes of Indo-Burman fold belt. Lalmai anticline outcrops in the delta and has a core of Pleistocene Brahmaputra sediment (BNGC013). Possible anticline where core B085 is located based on the presence of late Pleistocene Brahmaputra sediment is shown in red. The black box encloses the cores determined to have some Pleistocene Brahmaputra sediment in BNGB.

39

B. Holocene evolution of the Meghna valley

   i. Early Holocene

      a. Basinal muds

In the Meghna valley, the location and amount of terrestrial mud deposition is notable, because it cannot be explained by local overbank deposition because there are not associated sandy channel deposits.   Rather such thick mud units are known to indicate long term trapping of fine-grained sediments within the subsiding, seasonally flooded, and subsiding Sylhet basin. These basinal muds reflect backflooding of Sylhet basin associated with the post-LGM rise of sea level and increased sediment discharge with strengthened early Holocene monsoon, but given the absence of large sand bodies, indicate that they were not largely supplied by direct Brahmaputra input. Such a configuration is consistent with evidence for the Brahmaputra occupying its western, Jamuna course at this time (Goodbred and Kuehl, 2000; Pickering et al., 2013).

      b. Channel-levee sands

The absence of sandy channel deposits in the early Holocene valley fill indicates that neither the Brahmaputra occupied Sylhet basin course at this time nor were BSK sands escaping the subsiding Sylhet basin that was backflooded due to rising base level at this time. The BSK rivers have a sediment discharge today that is ~10% that of the Brahmaputra River, and the dimensions of ~10 km by 10 m thickness of the BSK channel deposits from the early Holocene imply that, when this river system is not joined by the Brahmaputra, it has more limited extent and lacks mobility over short timescales of 10^2-10^3 years. Although these BSK channel deposits are relatively small compared with those of the Brahmaputra braidbelt, they are neverltheless large when considering the 10-fold different in discharge between the two systems (fig. 16). These dimensions for the Holocene BSK deposits also differ from the 30-40 m thick BSK-sand packages that comprise the late Pleistocene stratigraphy, which can be explained as the

40

thicker Pleistocene deposits comprising stacked, amalgamated channel sequeunces similar to those recognized for the Brahmaputra along the Jamuna valley (Pickering et al., 2013).

ii.   Short occupation, 9.5 kyr BP

The 3-5 m thick deposits for the 9.5 kyr BP Brahmaputra occupation of the Meghna valley reflect a short duration and modest scale of sediment delivery to the Sylhet basin. When considering the nature of this avulsion from the main Brahmaputra channel, whether it was gradual or sudden and whether it was a full or partial avulsion can effect the size of the deposit. Based on the limited size of the sand body, we suggest that the channel-bed gradient along this Sylhet basin course must not have been favorable for sustaining a long-term avulsion. Thus, if it was not a hydrodynamically efficient course, then the cause of Brahmaputra avulsion at this time may have been an allogenic forcing, such as a flood or earthquake. For example, such events are know to have occurred during the Holocene, for example a large ice-dammed lake burst (Montgomery et al., 2004) and historic mega-earthquakes (Bilham and England, 2001).

iii.   Brahmaputra mid-late Holocene dominance

a.   Provenance of Holocene valley fill

Holocene Brahmaputra dominance in the Meghna valley depositing high Sr (>140 ppm) and high MS (>50 x 10^{-6}) is expected based on previous studies upstream and downstream of the Meghna valley, which show the Brahmaputra's immense sediment load as the driver of Holocene infill throughout the GBMD (Goodbred and Kuehl, 1999, 2000; Goodbred et al., 2003; Pickering et al., 2013; Goodbred et al., *in press*) (fig. 5). Holocene sediments in the main Meghna valley are almost entirely Brahmaputra or Brahmaputra influenced as shown by the extent and frequency of samples having high and mid Sr concentration and MS values (fig. 16). The Holocene valleys in BNGB and BNGC were infilled from the early Holocene to present by the Brahmaputra with few exceptions of input from smaller rivers and proximal sources (fig. 16). Brahmaputra influenced Holocene infill for several of the cores in the Meghna

41

valley in this study is as thick as 70 m (fig. 11, 16), which was constructed in as little as several thousand years in the Holocene.

Deposition in the Meghna valley during the Holocene is controlled by the episodic avulsion of the Brahmaputra River into and out of the Sylhet basin (Pickering et al., 2013). The Brahampura's high sediment discharge overcame the rapid sea level rise of >1 cm yr^{-1} coming out of the LGM and managed to begin progradation at 11.5 kyr BP occupying areas of the delta it was excluded from during the lowstand (Goodbred and Kuehl, 2000). Based on the dominance of BSK fluvial sediment input in the Pleistocene, the Meghna valley is one of the areas of the GBMD that the Brahmaputra was excluded from during the lowstand. During the Holocene highstand, and perhaps earlier highstands, the Brahmaputra makes prolonged connections with its old eastern course through Sylhet basin and the Meghna valley (fig. 4) (Pickering et al., 2013). The Brahmaputra is likely attracted to Sylhet basin due to subsidence that is mainly tectonically generated at a rate of 2-4 mm yr^{-1} through overthrust by Shillong Massif (Goodbred and Kuehl, 1999, 2000; Steckler et al., 2008). Despite Sylhet basin representing a local subsidence maximum for the GBMD, the Brahmaputra still spends much of the Holocene in its Jamuna course, only occupying the Meghna valley for one extended period in mid Holocene and two shorter-term, less well-constrained periods in the early and late Holocene (Pickering et al., 2013).

b.   Long Brahmaputra Holocene occupation 7.5-5 kyr BP

Brahmaputra braidbelt deposits infill the two sub-valleys that bisect the eastern edge of the Madhupur Terrace (fig. 16). Downstream where the Meghna valley widens, Brahmaputra braidbelt sediments are restricted to the western portion of the Meghna valley with thick, finer-grained deposits of the mixed Brahmaputra-BSK origin infilling the eastern Meghna valley synchronously (fig. 16). These Brahmaputra influenced-mixed sediment extend eastward to the fold belt margin along BNGB and to the western margin of Lalmai Anticline along BNGC (fig 16). The localization of Brahmaputra sands along the western Meghna valley indicate that the main braidbelt did not occupy the eastern portion of the

valley at any time during the Holocene. The location of the Brahmaputra braidbelt deposits constrains the extent of channel migration when the Brahmaputra occupied the Meghna valley during the Holocene long occupation from 7.5 to 5 kyr BP (fig. 16). The main channel must have been joined by the BSK channel to produce the amount of a mixed signal sediment that is found in the upper stratigraphy during this occupation (fig. 16). About 55% of total Holocene deposition takes place during the 7.5 to 5 kyr BP occupation, and there is no evidence in the sediment record afterwards that shows another Brahmaputra occupation. Deposition in the Meghna valley since the major Brahmaputra occupation is only from local sources on the valley flanks or channel deposits from the BSK river system is currently the main fluvial occupier of the valley (fig. 4, 6).

c.   Historical occupation

Following the major 7.5-5 kyr BP occupation of the Brahmaputra River in the Meghna valley, there is an historical occupation prior to early 19th century (Fergusson, 1863; Best et al., 2007). However, there is little clear evidence of this occupation in the sediment record of the valley. As recently as the late eighteenth century, only a couple hundred years ago, the Brahmaputra was in the Old Brahmaputra course which fed through the Meghna valley. This most recent occupation is suggested to have been relatively short, because of the lack of significant braidbelt sands deposited during this time. Such limited sand deposition during a known occupation event is similar to that recorded by the 9.5 kyr BP occupation (fig 16). The lack of evidence of this third avulsion into the Old Brahmaputra course calls into question how long the Brahmaputra needs to occupy a channel to show up in the sedimentary record and whether the problem of not recognizing it in the sediment record is a problem of not being able to distinguish the occupation because of the lack of deposition in between occupations. A lack of deposition in the last several thousand years seems plausible by examining the landscape in the eastern part of BNGB near the fold belt. There is an abandoned channel depression still visible that has yet to be fully filled in by sediment since its abandonment (fig 4, 6). The origin and history of this channel scarp remain uncertain, because the results from the cores do not reveal enough about this channel's recent abandonment.

d. Tectonic channel steering

Holocene braidbelt sands in BNGC with the highest Sr concentration and MS which is classified as Brahmaputra sediment is found in the westernmost part of the valley deposited onto Madhupur Terrace (fig 12, 13, 16). The concentration of Brahmaputra sediment on the western side of BNGC in a wide valley shows that the Brahmaputra is preferentially forced to that side of the valley. As seen upstream of the Meghna valley in both the Jamuna and Old Brahmaputra channels in BNGA, the Brahmaputra tends to occupy all locations of a valley over time with no preference in deposition to a particular part of the valley (fig. 5) (Pickering et al., 2013). In BNGC, it also appears that the Brahmaputra channel has eroded into Madhupur Terrace forming a bench-cut terrace that 30 m of Holocene Brahmaputra braidbelt deposition from the major occupation sits atop (fig. 16) for cores C073-081. The Pleistocene terrace below the braidbelt sand deposit is made up of low plasticity, desiccated muds that date back to the Pleistocene and correlate to the adjacent sediments to the west within Madhupur Terrace (fig. 16). Given the lack of structural constraints to the east, this 10 km wide, west lateral migration of the Brahmaputra River into the elevated Madhupur Terrace suggests that river course may have been steered by tectonic deformation of the Tippera surface at the edge of the advancing fold belt (fig 7, 16, 17) (Uddin and Lundberg, 2003; Sikder and Alam 2003).

From a DEM of SRTM data (fig. 4,6), the lateral gradient (S_l) from the fold belt to the modern channel location in the southern transect is measured to be 2.5×10^{-4} and the downstream gradient (S_d) is 1×10^{-4}, which puts S_l and S_d at the same order of magnitude with a ratio of 2.5 to 1 (fig. 7). From Peakall et al. (2000), as part of a study on avulsion and channel migration through tectonic tilting, the gradients were important but not the most important factor in how a fluvial channel will respond to tilting. The upstream-downstream and lateral gradients need to be on the same order of magnitude, but also the tilting rate needs to be high enough. For avulsion to occur the tilt rate needs to be greater than 5×10^{-4} rad kyr^{-1}, and the surface in the southern transect has an estimated Holocene tilt rate of 5.5×10^{-5} rad kyr^{-1} making this system more likely to experience channel migration than avulsion in response to the tectonic

tilting. From the Holocene-Pleistocene boundary and estimating that that surface has been tilting from horizontal since 110,000 years BP, an estimate Pleistocene tilt rate is 1.5×10^{-5} rad kyr^{-1} which makes it on the same order of magnitude as the Holocene tilt rate. These surface tilting rates are consistent with the interpretation that tectonic channel steering was responsible for erosion of the Brahmaputra into the western topographic barrier of Madhupur Terrace. The land surface of the tilted Tippera surface appears to have no evidence of fluvial channels recent enough to be recorded on the DEM, because no channel cuts appear in map view or cross section (fig. 6, 7). Tectonic channel steering in the Holocene was a controlling factor enough to keep the main channel on the western side of the valley against Madhupur Terrace with only Brahmaputra influenced mixed sediment filling in the upper stratigraphy from the main channel location of today to Lalmai anticline.

Chapter V

Conclusions

In this study for the Meghna valley over the late Quaternary, sediment provenance highlights fluvial channel dominance, anticlinal Pleistocene structures, Holocene channel occupations, and Holocene tectonic channel steering. Sediment provenance shifted in the late Pleistocene and early Holocene from being supplied by more local rivers that were part of the BSK river system that drains the Indo-Burman ranges to being mainly supplied by the Brahmaputra River, which accounts for the majority of sedimentation in the Holocene. From previous work, the provenance of the Meghna valley differs from the provenance upstream at the Jamuna-Old Brahmaputra avulsion node where sediment is supplied from the Brahmaputra both below and in the Holocene valley indicating Brahmaputra dominance as far back as the late Pleistocene onwards. The smaller BSK river system dominating the Pleistocene deposition in the Meghna valley leaves us wondering about the nature of the BSK river system during this time. In modern times, the BSK rivers deposits on the scale of several meters as part of meandering channel systems, which would lead us to believe the late Pleistocene sand deposits are an amalgamation of smaller channel-levee sand deposits. Places in the Meghna valley that do have Pleistocene Brahmaputra sediment, appear to be rare, older than the latest Pleistocene channel-levee sand deposits, and are linked to anticlinal folds. The center of Lalmai anticline is comprised of ~50 m of Brahmaputra braidbelt sands, while the western side of the BNGB has several cores with Pleistocene Brahmaputra sediments, which could be possibly part of the deformation continuing westwards with buried folding. These folds could be growing at a slow enough rate that they could be buried by a large amount of sedimentation coming out of the LGM, and yet the deformation could be leading to high enough tilt rates for the Brahmaputra to be excluded from the Meghna valley in the late Pleistocene. The Holocene occupation history of the Meghna valley by the Brahmaputra River of several occupations of varying time fits well with previous work in the GBMD. The 9.5 kyr BP occupation is recorded in the Meghna valley despite being brief and the extended occupation from 7.5 to 5 kyr BP is recorded to a much greater extent comprising the upper 30 m

of deposition of braidbelt sands. The most recent occupation was not found in the sediment record in the Meghna valley, which would indicate a short duration much like the 9.5 kyr BP occupation. The avulsion mechanisms and triggers are most likely varying for these different occupation times. The longer occupations come from a longer build-up of aggradation while the shorter ones could be forced by a tectonic event such as a lake burst flood or earthquake. As the deformation front continued to tilt the surface in the southeast of the Meghna valley giving the lateral gradient a higher gradient than the channel profile gradient, the channel was forced to migrate to the west during the Holocene which is seen in the Brahmaputra deposition during the 7-5.5 kyr BP occupation of the valley. Slight tilting of the land surface due to deformation alone managed to steer the main channel at least 50 km westwards during the Holocene. All of these findings coming from the determination of sediment provenance is quite promising for future work in the GBMD and other tectonically active basins with discernible and multiple inputs of sediment that are tectonically related. The methods used in this study work well as a first pass at identifying which areas of a basin need further study to answer the questions of how fluvial processes can effect tectonics and how tectonics can effect fluvial processes.

REFERENCES

Allen, M. B., and Davies, C. E., 2007. Unstable Asia: active deformation of Siberia revealed by drainage shifts. Basin Research, 19, 379–392. doi:10.1111/j.1365-2117.2007.00331.x.

Best, J.L., Ashworth, P.J., Sarker, M.H., and Roden, J.E., 2007. The Brahmaputra–Jamuna River, Bangladesh. In: *Large Rivers. Geomorphology and Management*. John Wiley & Sons, Ltd., 395–433.

Bilham, R., and England, P., 2001, Plateau "pop-up" in the great 1897 Assam earthquake. Nature, 410, 806–9, doi: 10.1038/35071057.

Broecker, W.S., Denton, G.H., Edwards, R.L., Cheng, H., Alley, R.B., and Putnam, A.E, 2010. Putting the Younger Dryas cold event into context. Quaternary Science Reviews, v. 29, p. 1078–1081, doi: 10.1016/j.quascirev.2010.02.019.

Burbank, D., Meigs, A., and Brozovic, N, 1996. Interactions of growing folds and coeval depositional systems. Basin Research, 8, 199–223. doi:10.1046/j.1365-2117.1996.00181.x.

Fairbridge, R.W. (Ed.), 1972. Encyclopedia of Geochemistry and Environmental Sciences. Van Nostrand-Reinhold, New York.

Fergusson, J., 1863. Delta of the Ganges. Q. J. Geol. Soc. Lond. 29, 321–354.

Garzanti, E., Andò, S., France-Lanord, C., Vezzoli, G., Censi, P., Galy, V., and Najman, Y., 2010. Mineralogical and chemical variability of fluvial sediments1. Bedload sand (Ganga–Brahmaputra, Bangladesh). Earth and Planetary Science Letters, 299, 368–381, doi: 10.1016/j.epsl.2010.09.017.

Glass, H.D., Frye, J.C., and Willman, H.B., 1964. Record of Mississippi River diversion in the Morton Loess of Illinois. Transactions Illinois Academy of Science, 57, 24-27.

Goodbred, S.L., and Kuehl, S.A., 1999. Holocene and modern sediment budgets for the Ganges-Brahmaputra river system: Evidence for highstand dispersal to flood-plain, shelf, and deep-sea depocenters. Geology, 27 , 559–562, doi: 10.1130/0091-7613(1999)027<0559:HAMSBF>2.3.CO;2.

Goodbred, S. L., and Kuehl, S. A., 2000. The significance of large sediment supply, active tectonism , and eustasy on margin sequence development : Late Quaternary stratigraphy and evolution of the Ganges – Brahmaputra delta. Sedimentary Geology, 133, 227-248.

Goodbred, S.L., Kuehl, S.A., Steckler, M.S., and Sarker, M.H., 2003. Controls on facies distribution and stratigraphic preservation in the Ganges – Brahmaputra delta sequence. Sedimentary Geology, 155, 301 – 316.

Goodbred, S.L., Youngs, P.M., Ullah, M.S., Pate, R.D., Khan, S.R., Kuehl, S.A., Singh, S.K., and Rahaman, W. *in press*. Piecing together Holocene stratigraphy of the Ganges-Brahmaputra-Meghna river delta using Sr sediment geochemistry: Implications for river behavior and delta evolution

Grimley, D. a., Follmer, L.R., and McKay, E.D., 1998. Magnetic Susceptibility and Mineral Zonations Controlled by Provenance in Loess along the Illinois and Central Mississippi River Valleys. Quaternary Research, 49, 24–36, doi: 10.1006/qres.1997.1947.

Holbrook, J., and Schumm, S.A., 1999. Geomorphic and Sedimentary Response of Rivers to Tectonic Deformation: A Brief Review and Critique of a Tool for Recognizing Subtle Epeirogenic Deformation in Modern and Ancient Settings. Tectonophysics 305, 287–306.

Jones, L.S. and Schumm, S.A., 1999. Causes of Avulsion: An Overview. *Fluvial Sedimentology VI*. Blackwell Publishing Ltd. 171-178.

Jones, R., and Beavers, A., 1964. Magnetic Susceptibility as an Aid in Characterization and Differentiation of Loess. Journal of Sedimentary Research, 34, 881–883.

Kim, W., Sheets, B. A., and Paola, C., 2010. Steering of experimental channels by lateral basin tilting. Basin Research, 22, 286-301. doi:10.1111/j.1365-2117.2009.00419.x.

Kimbrough, D., Abbott, P., Gastil, R., and Hamner, P., 1997. Provenance investigations using magnetic susceptibility: Journal of Sedimentary Research, 67, 879–883.

Leeder, M.R. and Alexander J., 2006. The Origin and Tectonic Significance of Asymmetrical Meander-belts. Sedimentology 34, 217–226.

Maher, B.A., Watkins, S.J., Brunskill, G., Alexander, J., and Fielding, C.R., 2009. Sediment provenance in a tropical fluvial and marine context by magnetic "fingerprinting" of transportable sand fractions. Sedimentology, 56, 841–861, doi: 10.1111/j.1365-3091.2008.00999.x.

Montgomery, D.R., Hallet, B., Yuping, L., Finnegan, N., Anders, A., Gillespie, A., and Greenberg, H.M., 2004. Evidence for Holocene megafloods down the Tsangpo River gorge, southeastern Tibet. Quaternary Research, 62, 201–207, doi: 10.1016/j.yqres.2004.06.008.

Nanson, G.C., 1980. A regional trend to meander migration. The Journal of Geology, 88, 100–108.

Oldham, R.D., 1899. Report of the great earthquake of 12th June, 1897. Mem. Geol. Surv. India 29, 377.

Ouchi, S., 1985. Response of alluvial rivers to slow active tectonic movement. *Geological* Society of America Bulletin, 96, 504–515.

Paola, C., and Martin, J.M., 2012. Mass-Balance Effects In Depositional Systems. Journal of Sedimentary Research, 82, 435–450, doi: 10.2110/jsr.2012.38.

Pate, R., Jr, S.G., and Khan, S., 2009. Delta double-stack; juxtaposed Holocene and Pleistocene sequences from the Bengal Basin, Bangladesh. Sed. Record, 7, 4–9.

Peakall, J., Leeder M., Best J., and Ashworth P., 2000. River Response to Lateral Ground Tilting: A Synthesis and Some Implications for the Modelling of Alluvial Architecture in Extensional Basins. Basin Research 12, 413–424.

Pickering, J.L., Goodbred, S.L., Reitz, M.D., Hartzog, T.R., Mondal, D.R., and Hossain, M.S., 2013. Late Quaternary sedimentary record and Holocene channel avulsions of the Jamuna and Old Brahmaputra River valleys in the upper Bengal delta plain. Geomorphology. doi: 10.1016/j.geomorph.2013.09.021.

Reid, J.B., 1992. The Owens River as a Tiltmeter for Long Valley Caldera, California. The Journal of Geology 100, 353–363.

Schumm, S.A., Dumont, J.F., and Holbrook, J.M., 2000, *Active Tectonics and Alluvial Rivers*, Cambridge University Press, New York, NY, 276 p.

Schumm, S.A., 2005, *River Variability and Complexity*, Cambridge University Press, New York, NY, 220p.

Sikder, A.M., and Alam, M.M., 2003. 2-D modelling of the anticlinal structures and structural development of the eastern fold belt of the Bengal Basin, Bangladesh. Sedimentary Geology, 155, 209–226, doi: 10.1016/S0037-0738(02)00181-1.

Singh, S., and France-Lanord, C., 2002. Tracing the distribution of erosion in the Brahmaputra watershed from isotopic compositions of stream sediments. Earth and Planetary Science Letters, 202, 645–662.

Singh, S.K., Kumar, A., and France-Lanord, C., 2006. Sr and 87Sr/86Sr in waters and sediments of the Brahmaputra river system: Silicate weathering, CO2 consumption and Sr flux. Chemical Geology, 234, 308–320, doi: 10.1016/j.chemgeo.2006.05.009.

Steckler, M.S., Akhter, S.H., and Seeber, L., 2008. Collision of the Ganges – Brahmaputra Delta with the Burma Arc : Implications for earthquake hazard. Earth and Planetary Science Letters, 273, 367–378, doi: 10.1016/j.epsl.2008.07.009.

Stuiver, M., and Reimer, P.J., 1993. Extended 14C database and revised CALIB radiocarbon calibraton program. Radiocarbon, 35, 215-230.

Uddin, A., and Lundberg, N., 2004. Miocene sedimentation and subsidence during continent–continent collision, Bengal basin, Bangladesh. Sedimentary Geology, 164, 131–146, doi: 10.1016/j.sedgeo.2003.09.004.

Zhang, W., Xing, Y., Yu, L., Feng, H., and Lu, M., 2008. Distinguishing sediments from the Yangtze and Yellow Rivers, China: a mineral magnetic approach. The Holocene, 18, 1139–1145, doi: 10.1177/0959683608095582.